Developmental Programming: Gestational exposure of sheep to a real-life environmental chemical mixture alters maternal metabolome in a fetal sex-specific manner

Thangaraj SV[1] 000-0003-4902-468X, Kachman M[2] 0000-0002-9996-8446, Halloran KM[1] 0000-0002-4050-1892, Sinclair KD[3] 0000-0002-6375-215X, Lea R[3] 0000-0002-6793-3601, Bellingham M[4] 0000-0002-3646-8989, Evans NP[4]0000-0001-7395-3222, Padmanabhan V[1]0000-0002-8443-7212

[1]Department of Pediatrics, University of Michigan, Ann Arbor, MI, USA

[2] MM BRCF Metabolomics Core, University of Michigan, Ann Arbor, MI, USA

[3]University of Nottingham, Sutton Bonington Campus, Loughborough, UK

[4]School of Biodiversity One Health and Veterinary Medicine, College of Medical, Veterinary and Life Sciences, University of Glasgow, UK

Disclosure statement: Authors have nothing to disclose.

Funding support for the publication includes: National Institute of Environmental Health Sciences R01 ES030374 (PV, LR, ENP), Michigan Lifestage Environmental Exposures and Disease (M-LEEaD) NIEHS Core Center P30 ES017885 (PV), Molecular Phenotyping Core, Michigan Nutrition and Obesity Center P30 DK089503. TSV is a Center Scientist in M-LEEaD NIEHS Core Center supported through P30 ES017885.

Corresponding Author
Vasantha Padmanabhan, MS, PhD
Department of Pediatrics, University of Michigan
7510 MSRB 1, 1500 W. Medical Center Drive,
Ann Arbor, MI 48109
Telephone: 734-647-0276
E-mail: vasantha@umich.edu

Abstract

Background: Everyday, humans are exposed to a mixture of environmental chemicals some of which have endocrine and/or metabolism disrupting actions which may contribute to non-communicable diseases. The adverse health impacts of real-world chemical exposure, characterized by chronic low doses of a mixture of chemicals, are only recently emerging. Biosolids derived from human waste represent the environmental chemical mixtures humans are exposed to in real life. Prior studies in sheep have shown aberrant reproductive and metabolic phenotypes in offspring after maternal biosolid exposure.

Objective: To determine if exposure to biosolids perturbs the maternal metabolic milieu of pregnant ewes, in a fetal sex-specific manner.

Methods: Ewes were grazed on inorganic fertilizer (Control) or biosolid-treated pastures (BTP) from before mating and throughout gestation. Plasma from pregnant ewes (Control n=15, BTP n=15) obtained mid-gestation were analyzed by untargeted metabolomics. Metabolites were identified using Agilent MassHunter. Multivariate analyses were done using MetaboAnalyst 5.0 and confirmed using SIMCA.

Results: Univariate and multivariate analysis of 2,301 annotated metabolites identified 193 differentially abundant metabolites (DM) between control and BTP sheep. The DM primarily belonged to the super-class of lipids and organic acids. 15-HeTrE, oleamide, methionine, CAR(3:0(OH)) and pyroglutamic acid were the top DM and have been implicated in the regulation of fetal growth and development. Fetal sex further exacerbated differences in metabolite profiles in the BTP group. The organic acid class of metabolites was abundant in animals with male fetuses. Prenol lipid, sphingolipid, glycerolipid, alkaloid, polyketide and benzenoid classes showed fetal sex-specific responses to biosolids.

Discussion:

Our study illustrates that exposure to biosolids significantly alters the maternal metabolome in a fetal sex-specific manner. The altered metabolite profile indicates perturbations to fatty acid, arginine, branched chain amino acid and one-carbon metabolism. These factors are consistent with, and likely contributes to, the adverse phenotypic outcomes reported in the offspring.

1. Introduction

Humans are exposed daily to a mixture of environmental chemicals, including endocrine disrupting chemicals (EDCs) such as bisphenol A, perchlorates, phthalates, per- and polyfluoroalkyl substances, all of which can interfere with normal homeostasis. Developmental exposure to these chemicals is believed to contribute to a range of non-communicable diseases such as obesity, type II diabetes, cardiovascular disease, male and female reproductive disorders, hormone-sensitive cancers, thyroid disruption, and developmental and neurological disorders [1-4]. The estimated annual economic burden and disease cost of the effects of EDCs is $340 billion in the USA [5], but this is likely to be an underestimate, as this data only relates to a small subset of EDCs.

Several studies have confirmed a direct relationship between individual EDCs and the manifestation of endocrine dysfunction with resultant adverse human health impacts [6-9]. These traditional single exposure studies, fail to reflect the 'real-life' scenario, which is characterized by exposure to chronic, low concentrations of mixtures of chemicals, studies of which are only recently emerging [10-12]. The Endocrine Society's recent statement on EDCs also recognizes this concern and has stressed the importance of transitioning EDC research from individual chemicals to mixture-research [1]. The emerging mixture studies are more often limited to specific classes of chemicals such as phthalates [13], heavy metals [14], and polyfluoroalkyl substances (PFAS) [15], or a small subset of compounds from these different classes [16-18], which still under-represents the real-world scenario. Some studies have used a combined

toxicological assessment and regression models to predict mixture-effects based on toxicodynamic assumptions [19-21]. However, environmental chemicals in a mixture can act by additive, antagonistic or synergistic mechanisms [22] in combination with other biotic and abiotic stressors [23], and the resultant health outcomes cannot be predicted by the above methods. These inherent challenges make the toxicological assessment of chemical mixtures using traditional approaches unreliable.

Biosolids are the by-product of treated sewage sludge generated during the domestic wastewater treatment process. They are rich in organic and inorganic plant nutrients and are extensively used in agriculture [24] and landscaping as an alternative to inorganic fertilizers. However, biosolids are also an environmental source of contaminants like microplastics [25], and they contain the array of chemicals humans are exposed to in real life [26], including PFAS [27] , phthalates[28], BPA[29] and other EDCs [30-32] all of which are present at environmentally representative concentrations [33,34]. Pregnant sheep grazed on biosolids-treated pastures (BTP) have measurable amounts of EDCs present in both adult and fetal tissues [35,36]. As sheep are a precocial species with fetal developmental timing similar to humans [37,38], sheep grazed on BTP represent an established and unique translationally relevant model to determine the effects of exposure to mixtures of environmentally relevant concentrations of environmental chemicals including EDCs with regard to physiological systems and health. Crops fertilized with biosolids have entered the human food chain. There is evidence on the accumulation of pharmaceuticals and personal care products in crop plants from biosolids treated soil [39], exposing another route through which biosolids affect humans.

There is mounting evidence that maternal insults during critical stages of fetal development can alter the epigenome [40] and transcriptome [41,42] and lead to long-term, sex-specific effects on offspring health [16,42-48]. Previous studies using the BTP sheep model have demonstrated adverse effects of gestational biosolids exposure on the fetus including changes in bone mineral density [49], disruptions within the fetal reproductive neuroendocrine axis [47,50,51], spermatogenic abnormalities and mixed testicular atrophy [52-54],

alterations within the ovarian proteome and genes involved in ovarian development [55,56], and increased thyroid weight [57]. Some of these studies also revealed sex-specific differences in the phenotypic outcome like the increase in thyroid gland weights was more pronounced in male fetuses [57] whereas decreased bone mineral density was observed in female fetuses [49]. The maternal metabolic environment is critical for normal fetal development [58] and metabolic programming [59]. Circulating metabolites such as pyruvate, lipids and amino acids act as important mediators of maternal-fetal communications as they are used to signal the needs of the developing fetus to the mother to effect physiological changes including increased uterine blood flow, muscle catabolism and enhanced glucose production [60]. The maternal metabolome could also reflect fetal sex-specific adaptations to environmental stressors, however, the mechanisms of this are poorly understood. The effects of environmental chemicals on the metabolome of pregnant ewes have not been characterized and an investigation of its potential disruption in BTP sheep will aid our understanding of the physiological and molecular responses to real-life environmental chemical-mixture exposure and observed phenotypic outcomes in the offspring of BTP ewes. Untargeted metabolomics is a high-throughput technology that detects thousands of small metabolites in biological specimens without prior knowledge of which metabolites may be present. It has recently been used in combination with other 'omic' technologies to provide evidence of exposure to xenobiotic mixtures [61-63] and disrupted endogenous metabolite profiles in response to their exposure [64-66]. We hypothesized that maternal exposure to biosolids will perturb the maternal metabolic milieu, in a fetal sex-specific manner, which may be linked to the adverse phenotypic outcomes in the offspring, evidenced in previous studies using this model [41,42,52-54,56].

2. Methods

2.1. Ethics statement: All the animals were maintained under normal husbandry conditions at the University of Glasgow Cochno Farm and Research Centre. All procedures were conducted in accordance

with the UK Home Office Animals (Scientific Procedures) Act 1986 regulations under license (PPL PF10145DF).

2.2. Animals: EasyCare ewes (*Ovis aries*) were maintained from 4 weeks prior to mating on pastures fertilized with either biosolids (BTP), at conventional rates (4 tonnes/ha, twice per annum, April/ September) or inorganic fertilizer supplying equivalent amounts of nitrogen (225 kg N/ha per annum) (control) [34,47]. The control and BTP pastures, while on the same farm, were over 1 kilometer apart from each other and were separated by both a dirt road and a stream ensuring separation of the animals. The pastures were at similar forage maturity and quality at the beginning of the study. Ewes were randomly allocated to the control or BTP groups. When fertilizers were applied, the sheep were kept off the pastures for at least 3 weeks as per UK legislation, after which animals were maintained on these pastures for the same length of time; any effect of season or timing of application are not relevant for the purpose of this study and likely to be minimal. Pre-conceptional maternal weight was not significantly different between the Control (68.5± 6.7 kg and BTP 70± 5.16 kg) groups. Ewes were mated by laparoscopic artificial insemination (AB Europe, Edinburgh UK) as per normal husbandry procedures. Briefly, the estrous cycle of ewes was synchronized by treatment for 12 days with intravaginal Chronogest CR sponges (MSD Animal Health UK ltd) followed by PMSG administration (400iu Intervet) on the day of sponge removal. The onset of estrus was facilitated by maintenance of ewes near the rams for 24 hours before artificial insemination. Semen from four rams, which had been maintained on control pastures, was used for artificial insemination of ewes from both control and BTP groups. A blood sample was collected from ewes on day 90 of gestation (which approximates mid-gestation of the 147-day gestation period in sheep), centrifuged, and the plasma harvested and stored at -20 °C. Plasma from pregnant ewes (Control, n = 15; BTP, n =15) were shipped on dry ice to the University of Michigan where it was received in a frozen state

within 6 days and stored at -80 °C until analysis. Analysis to determine potential effects of fetal sex was carried out using samples from ewes that carried either only male fetuses (control, n = 9; BTP, n = 5) or only female fetuses (control, n = 5; BTP, n = 7). Ewes with twin or triplet pregnancies with mixed sex fetuses were excluded from the fetal sex-specific analyses. Body condition score (BCS) of ewes (based on a 5-point scale: 1 = lean and 5 = obese) at parturition did not differ between Control (BCS = 2.2± 0.53) and BTP (BCS = 2.4± 0.51) groups.

2.3. Sample preparation: Plasma samples were removed from -80 °C storage and maintained on wet ice throughout the processing steps. To 100 µL sample, 400 µL of extraction solvent (1:1:1 Methanol: Acetonitrile:Acetone) containing internal standards was added. Samples were vortexed and incubated overnight at -20°C. Post incubation, the vortex step was repeated, and samples were centrifuged for 10 min at 14,000 RPM and 4° C to precipitate protein. From the supernatant, 200 µL was transferred to an autosampler vial and brought to complete dryness using a nitrogen blower in ambient conditions. Samples and controls were reconstituted with 100 µL of water: methanol (8:2 by volume).

2.4. Untargeted metabolite profiling: RPLC-MS was undertaken as described previously [67]. Briefly, samples were analyzed on an Agilent 1290 Infinity II / 6545 qTOF MS system with the JetStream Ionization (ESI) source (Agilent Technologies, Inc., Santa Clara, CA USA) using the Waters Acquity HSS T3 1.8 µ 100 mm column (Waters Corporation, Milford, MA). Each sample was analyzed twice, once in positive and once in negative ion mode. The injection volume for positive and negative mode was 5 µL and 8 µL, respectively. Source parameters were drying gas temperature 350°C, drying gas flow rate 10 L/min, nebulizer pressure 30 psi, sheath gas temp 350°C and flow 11 L/min, and capillary voltage 3500V, with internal reference mass correction.

2.5. Quality Control: Several quality control measures were employed. A pooled sample (a small amount of extract from each of the 30 samples) was run every ~5 samples to check for instrument drift during the run. The samples were randomized to avoid any bias by group. Isotopically labeled internal standards were present in the metabolite extraction solvent which could have been used for normalization in lieu of drift correction but was not needed. A long-term control Pooled Plasma (from bio reclamation) was run before and after the samples, to determine if missingness of named metabolites was due to instrument issue or if they were undetectable in our sample. Detection of all of the named compounds in this Long-Term Control ensured that all procedures in the preparation of samples and the LC-MS runs worked as expected.

2.6. Metabolite Detection: Identification of chromatographic peaks that represent features for this platform followed a hybrid targeted/non-targeted approach. Semi-quantitative data for known compounds was obtained by manual integration using Profinder v8.00 (Agilent Technologies, Santa Clara, CA.) Metabolites were identified by matching the retention time (+/- 0.1 min), mass (+/- 10 ppm) and isotope profile (peak height and spacing) to authentic standards. Non-targeted data detection was performed using Agilent's MassHunter Find by Molecular Feature workflow (v7.0) with recursion using Agilent's Mass Profiler Pro (v8.0).

2.7. Metabolite Data Cleaning and Degeneracy Removal: A pooled QC sample based robust 'locally estimated scatterplot smoothing' (LOESS) signal correction [68] was used to correct signal drift, batch effects, and to normalize the data, thus reducing systematic bias. A combined feature set was generated by merging untargeted features and named metabolites into a single feature list. The combined feature set

underwent data reduction using Binner [67]. Briefly, Binner performed RT-based binning, followed by clustering of features by Pearson's correlation coefficient, and then assigned isotopes, adducts or in-source fragments by searching for known mass differences between highly correlated features. In-house software was used to search Refmet (https://www.metabolomicsworkbench.org/databases/refmet/index.php) to provide MSI [69] Level III identifications, or to an in-house library of authentic standards to provide MSI Level I identifications.

2.8. Identification of unknowns: Iterative Data Dependent (iDDA) ms/ms analysis was performed on the pooled sample material. iDDA captures ms/ms in a stepwise fashion, with rolling excluded precursors. Five rounds of iDDA were performed at collision energy 20 and 40 for both positive and negative modes. At each collision energy, ~8000 ms/ms spectra were collected, which represents ms/ms spectra for approximately 75-95% of the features obtained by the untargeted data analysis. Analysis of iDDA spectra using NIST2020 was performed to provide MSI Level II identification for statistically significant features. Only validated (n=101 for Negative mode; n=140 for Positive mode) and putatively annotated (n=905 for Negative mode; n=1155 for Positive mode) features were used for further statistical analyses.

2.9. Statistical Comparison of Control and BTP Maternal Metabolome: Files with peak intensity values were uploaded to the online platform MetaboAnalyst (v5.0) [69] for analysis. The optimum handling of missing values in untargeted metabolomic analyses has been a subject of contention with several recommended workflows based on the type of data.[70-72] Features with over 50% missing values were removed from the analysis, the remaining missing values were estimated by K-Nearest Neighbours Algorithm imputation and features were filtered based on interquartile range to remove noise. This ensured that we did not remove features that were differentially missing between control and BTP groups that may be of biological importance. The feature values were log-transformed and auto-scaled [73] to minimize the

impact of noise and high variance of the variables. Comparisons were made between the control (n=15) and BTP groups (n=15) and fetal sex (Male: Control, n=9, BTP, n=5; Female: Control, n=5, BTP, n= 7).

Multi-dimensional statistical analysis was performed for the processed data using MetaboAnalyst5.0. Principal component analysis (PCA) was done to identify the principal components (PC), visualize the clustering, trends, and outliers in the data. In the BTP group, there were two outliers outside the 95% confidence region on the scores plot and they were removed from further analysis (Supplementary figure S1a). Orthogonal projections to latent structure discriminant analysis (OPLS-DA) was performed to identify differences in metabolic profiles and screen for differential metabolites responsible for the differentiation between control and BTP groups. PCA and OPLS-DA are distinct modeling frameworks that accomplish different goals and extract different information from metabolomics data [74] and hence we present both PCA and OPLS-DA analysis alongside each other as commonly represented in many metabolomic studies. [75,76] The OPLS-DA scores plot showed the distribution of the two groups. The robustness of the model is indicated by the Q^2 and R^2Y values represented in the Q^2/R^2Y overview plot. The R^2Y gives goodness of fit and Q^2 gives the predictive ability of the model. Models with Q^2 and R^2Y values >0.5 were considered stable and reliable models [77]. To avoid overfitting of the OPLS-DA models, random permutation testing with 100 permutations was done. As some of the models had lower Q^2 values, we also performed PCA and OPLS-DA analyses using SIMCA version 17 (Umetrics, Sweden) and confirmed the models using a permutation test with 100 permutations. The variable importance in projection (VIP) plot derived from OPLS-DA was used to identify the metabolites that contributed the most to the model. A VIP cut-off value of 1.0 was used to select important features [78]. Since independent metabolite differences may complement each other, which cannot be reflected in a univariate analysis [79], significantly different metabolites were obtained based on the criteria that, FDR adjusted, Student's t-test P value < 0.05 and VIP > 1. The heatmap was constructed based on the top metabolites of importance

identified by Student's t-test. The differential metabolites were matched to metabolomics pathways using the Pathway Analysis and Enrichment Analysis feature in MetaboAnalyst. Pathways were considered significantly enriched if $P < 0.05$, impact 0.1 and number of metabolite hits in the pathway ≥ 2. For the class analysis of metabolites, log-transformed, scaled peak-intensity values of the differential metabolites were used. An unpaired Mann-Whitney U test was used to test for significance between the control and BTP groups. Benjamini-Hochberg adjusted P value <0.05 was considered significant. Two-way ANOVA with Tukey's post hoc test with alpha value set to 0.05 was used for inter-group comparisons of fetal sex in the two groups. Bar graphs were generated using GraphPad Prism 9.4.1(GraphPad Software,Inc., San Diego, CA).

2.10. Correlation Network Construction: MetaboAnalyst 5.0 web-tool was used to construct a De-Biased Sparse Partial Correlation (DSPC) network based on the differential metabolites. The nodes indicate the metabolites, and the edges represent the partial correlation coefficients. The default DSPC network only showed the top correlation based on their P value ranking.

3. Results:

3.1. Metabolite profiling in control and BTP groups: Using the untargeted metabolomics approach, the negative ionization mode identified 2,548 metabolites comprising 1,006 known metabolites and 1,542 unknown metabolites while the positive ionization mode identified 3,675 metabolites, including 1,155 known metabolites and 2,520 unknown metabolites. Only known metabolites were used for further analysis. An unsupervised PCA revealed intrinsic variations within the data and reduced the dimensionality of the data. In the negative ion mode, PCA scores showed that PC1 and PC2 were responsible for 17.4% and 13.3% of the variation respectively. In the positive ion mode, PCA scores

showed that PC1 and PC2 were responsible for 15.5% and 13.9% of the variation respectively. The PCA indicated a moderate separation between the control and BTP groups (Figure 1- top). A supervised OPLS-DA showed a strong clustering of the control and BTP groups based on metabolite abundance (Figure 1 bottom). The OPLS-DA model generated had a R^2Y value of 0.88 and Q^2 score of 0.74 in the negative ion mode and a R^2Y value of 0.79 and Q^2 score of 0.71 in the positive ion mode, indicating a robust model with good fit and predictive power. The validation of the OPLS-DA model by permutation test confirmed that the models were not random or over-fitted and the differences between the groups within the model were highly significant. This was confirmed by the models in SIMCA with high R^2Y and Q^2 values (Supplementary figure S1b).

3.2. Impact of biosolids exposure on metabolites: Students t-test identified 92 and 123 differentially abundant metabolites in the BTP group compared to the controls, from the negative and positive ion modes, respectively. A heatmap of the top 25 significant differential metabolites, indicated variable pattern of abundance of the metabolites in control and BTP groups in the negative and the positive modes (Supplementary figure S2a). OPLS-DA identified 210 and 279 metabolites with VIP>1 that differentiated the control and BTP groups from negative and positive ion modes, respectively. The top 25 metabolites with highest VIP from the negative and positive modes and their direction of change in the control and BTP groups are represented in the VIP Score plot (Supplementary figure S2b). After removing duplicate entries between the two modes, a total of 193 metabolites were identified as differential metabolites (DM) between the control and BTP groups (Supplementary Table S1). The top 10 DM from the negative and positive modes are listed in Table 1.

3.3. Metabolite classes impacted by biosolids exposure: The 193 differential metabolites between control and BTP groups were organized into 10 classes, the proportions of which are shown in Figure 2a. The sub-class distribution of differential metabolites belonging to the top 2 classes: Lipid and lipid-like molecules (75) and organic acids and derivatives (59) are represented in Figures 2b and 2c, respectively. Lipid and lipid-like molecules primarily included fatty acyls and glycerophospholipid sub-classes, while the organic acids and derivatives class majorly included amino acids, peptides and analogues sub-classes. The other classes each of which represented between 5% and 10% of the differentially abundant metabolites included organoheterocyclic compounds (20), benzenoids (15) and nucleosides, nucleotides and analogs (10). Pathway analyses revealed that the valine-leucine-isoleucine biosynthesis, aminoacyl t-RNA biosynthesis and phenylalanine, tyrosine and tryptophan biosynthesis pathways were enriched in the BTP group (Figure 2d).

Levels of abundance of the different classes of the differential metabolites that were significantly different between the control and BTP groups are represented in figure 3. Overall, among the lipids, fatty acyls (FA), prenol lipids (PL) and sphingolipids (SL) were present at a significantly lower level, while glycerophospholipids (GPL) and glycerolipids (GL) were present at a higher level in the BTP group. The pattern of expression of different sub-classes of lipids between the different groups is represented in a heatmap in supplementary figure S3. The next major class of differential metabolites, organic acids and derivatives, which primarily comprised of amino acids and peptides, showed an overall decreased abundance in the BTP group (Figure 3, Supplementary figure S4). Nucleosides, nucleotides and analogues class of differential metabolites were increased due to BTP exposure (Figure 3, Supplementary figure S5a). BTP exposure was also associated with reduced levels of the alkaloid class of metabolites but increased levels of phenylpropanoids and polyketide metabolites (Figure 3, Supplementary figure S5b and c). Organic compound classes like organoheterocyclic, organic nitrogen, organic oxygen and organosulfur

compounds showed a decreasing trend in the BTP group (Supplementary figure S5d), but the effect was not statistically significant. Benzenoids were elevated in the plasma of BTP animals (Figure 3, Supplementary figure S6 top). Analyzing the different sub-class of lipids, the fatty acyl class consisted of differential metabolites from fatty acid, acyl carnitines and fatty amide sub-classes. Long chain fatty acids like sebacic acid and 15-HeTrE were lower, while dodecanedioic acid, eicosanedioic acid, and eicosapentanoic acid were higher in the BTP group (Figure 4a). Relative levels of 14 acylcarnitines were lower in the BTP group (Figure 4b). Among the fatty amides, oleamide and palmitamide levels were higher and S-(2-Methylpropionyl)-dihydrolipoamide-E was lower in the BTP group (Figure 4c). Similarly, within the organic acids and derivatives class, the branched chain amino acids - valine, leucine and other amino acids including methionine, tyrosine, citrulline, creatinine, ornithine, alanine, homoarginine and phenylalanine were present at higher levels in the BTP group (Figure 5, Supplementary table S2). Summary statistics for all comparisons of metabolite expression between control and BTP groups with P values are listed in supplementary table S2. In general, the data implies specific patterns of differences in metabolite levels associated with exposure to BTP.

3.4. Exogenous metabolites: The identified differentially abundant exogenous metabolites were small molecules derived from drugs, food, microbes, synthetic compounds in personal care products that are not part of natural biology of the source organism. The 41 differential exogenous metabolites identified in the BTP group are listed in supplementary table S3. Of these, (2-Chlorophenyl) diphenylmethane, 10-nitrooleic acid, 2- amino hippuric acid, octadecatrienoic acid, biotin sulphate, cartap, 7-aminocephalosporanic acid and phosphonoacetaldehyde have been identified as part of the human exposome. The differentially abundant exogenous metabolites also included the microbial metabolites

benzoic acid, threonic acid, citramalic acid and O-demethylpuromycin. The other exogenous metabolites were largely identified as metabolites derived from food and drugs.

3.5. Correlation Network: Differential endogenous and exogenous metabolites were used to construct De-Biased Sparse Partial Correlation Network (DSPC) to investigate potential interaction and regulation among all metabolites. The correlation subnetworks constructed identified dense positive interactions between exogenous metabolites of the benzenoid family and the organic acid derivatives (phenylacetylglycine and phosphonoacetaldehyde), fatty acids (dodecanedioic acid, nucleotide analogue - 7-methylxanthosine) and the organic compound midazolam. (Supplementary figure S6 bottom).

3.6. Potential Biomarkers: The OPLS-DA model S-plot, VIP score and t-test were used to identify potential signatures of BTP exposure (Figure 6). 15-HeTrE, oleamide, methionine, GTOL, tetraphenylphosphonium, ornithine and lysine were the metabolites that showed increased levels in the BTP group. The metabolites CAR (3:0(OH)), pyroglutamic acid, cartap, N-Decanoyglycine, Arg-Ile-Pro and 5-O-Methylvisamminol showed lower levels in the BTP group.

3.7. Effect of fetal sex on metabolites: Within control and BTP groups, comparison of the metabolome of ewes carrying male or female fetuses using unsupervised (PCA) and supervised multivariate analysis (OPLS-DA), revealed no significant clustering of metabolites. However, when animals were stratified based on fetal sex and the metabolome of control and BTP groups was compared, sex-specific effects of biosolids treatment on the metabolome were apparent. In ewes carrying male fetuses, moderate grouping was seen between BTP, and control ewes based on multivariate analysis of metabolites. PCA scores showed that PC1 and PC2 were responsible for 29.6% and 16.7% of the variation respectively. In the

positive ion mode, PCA scores showed that PC1 and PC2 were responsible for 25.4 % and 17.8% of the variation respectively (Figure 7a- top). The PCA did not reveal a clear separation between control and BTP groups. However, the OPLS-DA model generated (Figure 7a- bottom) had a R^2Y value of 0.75 and Q^2 score of 0.40 in the negative ion mode and a R^2Y value of 0.81 and Q^2 score of 0.40 in the positive ion model. In ewes carrying female fetuses, a clear grouping of control and BTP groups was evident by both univariate and multivariate analyses. In the negative ion mode, PCA scores showed that PC1 and PC2 were responsible for 19.9% and 16% of the variation respectively. In the positive ion mode, the PCA scores showed that PC1 and PC2 were responsible for 22.9% and 17% of the variation respectively (Figure 7b- top). The PCA indicated a moderate separation between control and BTP groups. The OPLS-DA model generated (Figure 7b- bottom) had a R^2Y value of 0.93 and Q^2 score of 0.68 in the negative ion mode and a R^2Y value of 0.88 and Q^2 score of 0.58 in the positive ion mode, indicating a robust model with good fit. The confirmation models derived from SIMCA software are included in the supplementary (Supplementary figure S7).

From fetal sex-specific analyses, in ewes carrying male fetuses, univariate analysis comparing control and BTP ewes identified 15 metabolites that were differentially abundant, with the top 5 being Oleamide, Tetraphenylphosphonium, Pyroglutamic acid, 5-Hydroxytryptophol glucuronide and Arg-Ile-Pro (Supplementary Table S4, Supplementary figure S8). From ewes carrying female fetuses, a total of 83 differential metabolites were identified with the top 5 being 15-HeTrE, alpha-cyclohexylmandelic acid, aflatoxin B1 dialcohol, MG (17:0), and CAR (DC6:0) (Supplementary Table S5). The heatmap based on the top 25 significant metabolites based on a t-test indicated variable pattern of expression of the metabolites in control and BTP groups (Supplementary figure S9a). The VIP score of the top 25 metabolites from the OPLS-DA models, and heatmap showing the direction of change are represented in the VIP Score plot (Supplementary figure S9b).

The fetal sex-specific expression of the different classes of the differential metabolites that were significantly different between the control and BTP groups are represented in figure 7c. Metabolites of the alkaloid class and the lipid sub-classes, prenol lipid and sphingolipid classes of metabolites were significantly different between the control and BTP groups only in animals with male fetuses, whereas the levels of polyketides, benzenoids and glycerolipid sub-class of metabolites was different between the treatment groups only in animals with female fetuses. The benzenoid class of metabolites also had a significant interaction between the treatment and fetal-sex effects based on ANOVA. The organic acids and derivatives class of metabolites showed fetal-sex specificity with higher levels of organic acids in ewes carrying male fetuses of both control and BTP groups. Summary statistics for all comparisons of metabolite expression between control and BTP groups based on fetal sex are listed in Supplementary table S6.

4. Discussion:

The current study used an untargeted metabolomics approach and provided evidence that exposure to 'real-life' low dose mixtures of environmental chemicals from grazing on BTP prior to conception and throughout gestation, perturbs the maternal metabolome during mid-pregnancy in sheep. The 193 differentially abundant metabolites identified in the plasma of BTP ewes included several environmental chemicals and endogenous metabolites that are known to affect fetal development, including oleamide, pyroglutamic acid and 15-HeTre. The majority of the differentially abundant metabolites were either lipids and lipid-like molecules or amino acids and their derivatives. Importantly, the sex of the fetuses further exacerbated differences in metabolite profiles in the BTP group. Although BTP ewes with male fetuses showed differences in their metabolite profile compared to control ewes, BTP ewes carrying female fetuses showed a greater number of differences in their metabolite profile compared to control ewes.. Overall, the results suggest a previously unappreciated impact of exposure to low level chemical mixtures

on the maternal metabolome, which could have potential implications for fetal development. The relevance of the differential metabolites to the previously observed phenotypic changes in the BTP offspring including changes in spermatogenic and oocyte development, altered bone mineral density, increased thyroid organ weight and reproductive-neuroendocrine systems [36,47,49-53,55-57] are discussed below.

4.1. Multiple lipid species altered by biosolids exposure: Maternal lipids are major determinants of fetal development and offspring health. [80,81] It is therefore of interest that 38% of the metabolites that were differentially present in BTP mothers were lipids and lipid-like molecules. The contribution from different lipid sub-classes is an essential consideration when studying the impact of perturbations in maternal lipid metabolism. The fatty acyl sub-class, which comprised over half of the lipid molecules that were altered in the BTP group, included fatty acids, acylcarnitines and fatty amides. Levels of the long chain fatty acids dodecanedioic acid, eicosapentanoic acid and eicosanedioic acid were increased, while sebacic acid and 15-HeTre were decreased in the BTP group compared to the controls. Maternal plasma fatty acids are involved in cell growth, signaling and development and are therefore key to normal fetal development and developmental programming [82,83]. Essential fatty acids and polyunsaturated fatty acids are used by the developing fetus to maintain plasma membrane dynamics, as an energy source and as a precursor for bioactive compounds [84]. Hence disrupted patterns of fatty acids and polyunsaturated fatty acids in the maternal metabolome of BTP ewes could have far reaching consequences for fetal health. Indeed, impaired fatty acid metabolism has previously been shown to adversely affect oocyte development [85] and spermatogenesis [86]. Acylcarnitine sub-class of metabolites, which transport long-chain fatty acids into the mitochondria for β-oxidation and are critical for energy production to sustain cellular activity [87], were

lower in the BTP group compared to the controls, suggesting the BTP sheep may have impaired β-oxidation [88], which could negatively affect growth and development of the fetus [89].

The BTP sheep also had altered levels of fatty amides, which are bioactive, endogenous signaling molecules that regulate various cellular and physiological functions [90]. The fatty amide methylpropionyl dihydrolipoamide, an intermediate in branched-chain amino acid degradation [91], was increased in BTP sheep. The fatty amides oleamide and palmitamide, which were elevated in BTP sheep, are known to interact with the endocannabinoid receptors [92,93], which is associated with fetal health, [94] oocyte development [95] and maturation [96], regulation of bone formation and bone mass [97], regulation of the reproductive- neuroendocrine axis [98] and spermatogenesis [99]. Animals in the BTP group also had increased glycerolipids, the storage form of fatty acids in adipocytes [100], and glycerophospholipids - key components of the lipid bilayer of cells. Increased glycerophospholipid metabolites in pregnancy, as seen in the BTP sheep, are associated with decreased methylation of genes related to fetal development[101] and hence could have a long-lasting impact on fetal health. BTP ewes also had decreased levels of sphingolipids, the bioactive membrane lipids which regulate angiogenesis in the placenta [102] and bone remodeling [103]. This is of specific interest since offspring of BTP sheep exhibit disrupted bone homeostasis [49]. Similar results showing disrupted fatty acid metabolism in response to EDC exposure have also been reported in metabolomic studies in humans [104].

In addition to lipid metabolites, other metabolites involved in fatty acid metabolism were also impacted by BTP exposure. For instance, higher levels of 2-methyl hippuric acid and hydroquinone, which are biomarkers for internal exposure of benzene [105,106] and associated with disturbed fatty acid oxidation [107] were evident in the BTP group. Among the differentially abundant metabolites in the BTP sheep were 13 established markers of inborn errors of metabolism, namely, citrulline, inosine, phenylalanine, acetylserine, ornithine, pyroglutamic acid, sebacic acid, succinyladenosine, uridine, valerylglycine,

hexanoylglycine, aminoadipic acid and phenylacetylglycine. Inborn errors of metabolism are caused by dysfunction in pathways within cellular organelles like mitochondria [108] and are indicative of disrupted lipid metabolism. Additionally, two of these differential metabolites, hexanoylglycine [109] and phenylacetylglycine [110], have previously been used to diagnose disorders of mitochondrial fatty acid β-oxidation in humans. Another metabolite that had lower levels in the BTP sheep, pantothenic acid (Vitamin B5), is known to play an important role in fatty acid synthesis and β-oxidation [111] and is essential for normal fetal growth, as its deficiency in maternal plasma is associated with poor birth outcomes in offspring [112]. The observed changes in the lipid profile are reflective of changes in fatty acid metabolism that may have contributed to the phenotypic changes reported earlier in the BTP model. [41,42,52-54,56].

4.2. Multiple amino acid pathways are influenced by biosolids exposure: Organic acids that primarily included amino acids (AA) comprised a large portion of the maternal metabolome affected in the BTP sheep. AA play a key role in placental and fetal development and any disturbances in maternal AA levels could compromise whole body homeostasis and fetal growth [113]. EDCs can compromise maternal amino acid balance, as evident from earlier studies that have found increased levels of arginine, tyrosine, phenylalanine, methionine, leucine, and valine in the maternal circulation following exposure to phthalates [114]. Similarly, we found components of the arginine metabolic pathway including citrulline, ornithine, homoarginine, creatine, and creatinine to be reduced in BTP sheep, which may provide a link to the alterations in gonadal development previously described [53,56,115]. Homoarginine metabolism has been implicated in normal ovarian folliculogenesis [116], and decreased levels of homoarginine in BTP sheep may have contributed to the altered proportions of fetal ovarian follicles [115] and aberrant gene and protein expression in oocytes [56,115] of BTP offspring. Disruption of arginine metabolism, through ornithine and citrulline, may also be implicated in the testicular dysgenesis-like phenotype seen in BTP offspring [53], as

metabolites of arginine are important for spermatogenesis, sperm quality, and male fertility [41,52,53,117,118] .The increase in tyrosine accompanied by the decrease in its precursor, phenylalanine in the BTP sheep could be functionally important as altered plasma tyrosine levels is suggested to impact thyroid function.[119] Previous reports indicate BTP exposure results in outcomes related to the delayed thyroid development [57], which could be related to the altered maternal phenylalanine-tyrosine metabolism [57] and thyroid function [119].

Exposure to BTP also had an impact on one-carbon metabolism, that manifested as an increase in methionine, betaine, and pyridoxamine (a form of vitamin B6). One carbon metabolism is important to generate products for synthesis of nucleic acids [120] and S-adenosylmethionine (SAM), which is the primary methylating agent for epigenetic modifications that occur during pregnancy [113,121,122]. In pregnant sheep, methionine levels start to rise at mid-gestation in maternal plasma [123], supportive of the importance of methionine and one carbon metabolism for fetal development.

Finally, the branched chain amino acids (BCAAs) metabolism involving the amino acids leucine, isoleucine, and valine was one of the top differential pathways identified in this study, with higher levels of BCAA seen in plasma of BTP sheep. BCAAs influence arginine metabolism and one carbon metabolism, are involved in the regulation of bone mineral density [124], and shares links with lipid metabolism [125] indicating their requirement for a wide variety of roles in the body [126,127]. Also, altered BCAA and/or lipid metabolism as seen in the BTP sheep, is characteristic of programming of metabolic disease[128]. Unpublished data from our group indicates that hypothalamic expression of markers related to energy balance and lipid metabolism are perturbed in prepubertal offspring of BTP sheep, while post-pubertal males have increased backfat thickness.

The potential markers of BTP exposure identified in this study- oleamide, 15-HeTrE and pyroglutamic acid have been implicated in fetal growth and development. 15-HeTre modulates

arachidonic acid metabolism [129] and upregulates PPARγ expression [130], factors that are associated with fetal programming[131,132]. Pyroglutamic acid is an intermediate in glutathione metabolism and oxidative stress regulation [133], in addition to playing an essential role in ovarian development [134]. The elevation in phenyllactic acid in BTP sheep, which is a metabolic biomarker for phenylketonuria [135] and a contributor to oxidative stress [136], is suggestive of increased oxidative stress in the BTP mother. Phenylalanine [137], hydroquinone [138], allantoin [139], which were present at higher levels in the BTP group, are also established oxidative stress markers. The possibility that BTP mothers were subject to higher levels of oxidative stress is also supported by the observation that BTP ewes had higher levels of BCAA that is known to promote oxidative stress [140] and lower levels of bilirubin and its metabolic precursor biliverdin which are proposed to have antioxidant activities [141].

Overall, the biology of the identified differential metabolites in BTP sheep collectively point towards disrupted fatty acid oxidation and increased lipid storage, which are features associated with chronic oxidative stress in pregnancy.[142] Fatty acid oxidation disorders result in the accumulation of oxidation substrates which leads to pathological levels of oxidative stress resulting in disturbed mitochondrial respiratory chain and energy production.[143] Oxidative stress as a consequence of environmental chemical exposure is well documented [144-147] and has been identified as one of the hallmarks of environmental insults [148]. Elevated oxidative stress is speculated to alter normal placental osteogenic signaling and fetal skeletal formation [149]. Maternal oxidative stress also interferes with normal oogenesis [150], ovarian follicular growth and development [151,152], spermatogenesis [153], and reproductive indices [154] in the fetus. Hence, oxidative stress response to BTP exposure may have contributed to the phenotypic changes seen in the offspring of the BTP sheep model including altered bone density, ovarian and follicular development, spermatogenesis and fetal growth [41,42,52-54,56], an aspect that remains to be investigated.

4.3. Fetal sex-effects on the maternal metabolome: Our study indicates that BTP animals carrying female fetuses exhibited more significant changes in the maternal metabolome, compared to animals with male fetuses. While it is well established that maternal metabolites are important factors for maternal-fetal communication, [60] and sex-specific differences in fetal responsiveness to changes in maternal milieu exists [155] the converse, namely impact of fetal sex on maternal metabolome is not well studied. Recent studies have highlighted that some maternal lipids [156] and their gestational stage-specific distribution [157] differed by fetal sex, although the underlying mechanism is unknown. In our study, we found the organic acid class of metabolites to be higher in animals with male fetuses. There is evidence of differential distribution of fatty acids and amino acids between maternal plasma and cord blood, [158] [159] suggestive of differential intrauterine nutrient transfer. An earlier study reported fetal sex-specific differences in placental uptake of unsaturated fatty acids in obese women [160,161]. Nutrient handling and transport of metabolites to the fetuses by the placenta could be sex-specific leading to sex-specific differences in the maternal metabolomic profile. It has been suggested that in women with normal glucose tolerance [162] and diabetes[163], women carrying a female fetus have lower fasting plasma glucose concentrations compared to those bearing a male fetus. Fetal sex is also known to influence the maternal steroidal milieu[164]. In this context, our findings suggest that fetal sex influences the maternal metabolome, the precise mechanism of which needs to be investigated. Fetal sex-specific maternal metabolic response to BTP-exposure that affected only animals carrying fetuses of a particular sex were evident in the concentrations of certain lipid sub-classes, alkaloids, polyketides and benzenoids. Additionally, the benzenoids class of metabolites show a significant interaction between the treatment and fetal-sex effects. Studies on sex-specific differences on placental and maternal metabolomes are only emerging and further paired studies

comparing maternal and fetal/placental metabolome at different timepoints will provide better insights into the effect of fetal sex on the maternal metabolome.

4.4. Strengths: Ours is the first proof of concept study to apply metabolomics to validate the effect of real-life environmental chemical exposure at environmentally relevant concentrations in a large animal model. Metabolomics provides a molecular snapshot of the subject in response to an environmental exposure, providing avenues to identify potential biomarkers of environmental chemical exposure and perturbed biological mechanisms [66,165,166]. Several studies have utilised metabolomics to identify the health implications of exposure to environmental pollutants such as microplastics [167], heavy metals [168], cadmium [169], particular matter [170], trichloroethylene [171], manganese [172], bisphenol A [173] and PFAS [174]. However, metabolomic studies are lacking in the area of the effects of environmental chemical mixtures with the exception of a cohort study on mixed environmental exposure response [175]; consequently our study contributes towards helping fill this gap in knowledge. As the sheep is an outbred, translationally relevant animal model which has a developmental trajectory similar to humans, our study offers a realistic assessment of risk to human health. With the widespread use of biosolids in agriculture for crop and animal production, its use for land remediation, and for golf courses and domestic use (lawns and gardens), humans are also at risk of exposure to the various chemicals present in biosolids.

4.5. Limitations: Th**e** major limitation of this study, as with other untargeted metabolomics studies, is the large number of unknown features that are absent from the metabolomics database [176] and hence not annotated. Metabolite identification is intrinsically difficult owing to the chemical complexity and diversity of metabolomes [177]. Unfortunately, the sheep plasma metabolome lacks representation in public

555 databases. We attempted to overcome this limitation through the use of alternative data dependent analysis
556 for further identification of unknowns. Another caveat of untargeted metabolomics is that the number of
557 samples is greatly outnumbered by the number of variables analyzed, which can lead to problems in
558 statistical analysis, and the reporting of false positives which can lead to erroneous biological conclusions
559 [178,179]. To combat this, we have used stringent criteria including two parameters, namely VIP score and
560 false discovery rate adjusted P values to identify differentially abundant metabolites. Although supervised
561 approaches like OPLS-DA have a tendency to over-fit data, through the identification of separate classes
562 even in the absence of real distinction between them, we have used permutations to test for the significance
563 of class separation and confirmed our results using a second tool (SIMCA). Also, our R^2Y and Q^2 values
564 were comparable, a parameter that shows the pertinence of the OPLS-DA model [180]. As the
565 MetaboAnalyst software used only a small subset of the differential metabolites that were mapped to
566 HMDB and excluded the lipids for the pathway analysis, this could have introduced a bias in analysis and
567 lead to an incomplete picture of the pathways affected. Hence, we looked at the functional role of each of
568 the metabolites and related them to the pathways they are involved in. Within the data set obtained in this
569 study we noticed large inter-animal variability in the level of metabolites. This could suggest that not all
570 animals were equally exposed (e.g., due to differences in grazing patterns or biosolids distribution) or that
571 they do not all respond equally to biosolids exposure. Although this is an analytical complexity, we feel
572 that it is also a strength of the model as it more truly reflects the real-world scenario where every individual
573 is exposed to different combinations and concentration of chemicals and due to individual differences may
574 respond differently to the insult they are exposed to.
575
576 **4.5.1. Challenges of working with Biosolids:** Working with biosolids has several technical limitations
577 compared to conventional chemical mixtures. It is difficult to give a toxicological assessment of biosolids

as the composition is likely to vary from location to location and even between batches at the same location. However, this reflects real-life exposure in humans, as no one is exposed to the same set of chemicals at the same level. Although a study supported by the U.S. Environmental Protection Agency has recently documented a list of 726 chemicals present in biosolids [181], it is not practical to document the exact composition and concentrations of hundreds of chemicals that constitute the biosolids used in our study. Earlier publications have documented the chemical makeup of biosolids used at that time within this model. [36,182] The difference between the concentrations of biosolids in the soil, within the plant, or on the surface of the grass was not assessed in this study. However, it is likely that water soluble compounds will be taken up by the root of the grass and deposited within the grass blades, while lipophilic compounds will remain on the surface of the plant [183] and the grass (and some soil containing biosolids) are ingested by sheep. Apart from ingestion, other routes of exposure of sheep to biosolids includes inhalation and absorption[31]. Additionally, sheep have ruminal microbes that could process some compounds found in biosolids into other forms, which could not be accounted for in this study. Although care was taken to ensure that the total nitrogen content was the same for both the biosolids treated and the conventional fertilizer pastures, as nitrogen is usually the rate limiting nutrient for crop production [184], the different types of fertilizer could impact the micro/macro nutrient content of the grass that may have contributed to differences in the metabolome. This, however, would be true when comparing any two types of fertilizer with different compositions.

4.6. Future directions:

With fatty acid oxidation and oxidative stress emerging as key pathways perturbed in this study, we will investigate markers of these two pathways in control and BTP tissues and plasma samples to confirm our findings. To confirm the effects of these metabolites on fetal programming, we will undertake detailed phenotyping of the offspring of BTP animals. The epigenome is reflective of environmental

exposures with epigenetic marks serving as biomarkers of exposure[185], and the metabolomics results need to be correlated with the epigenomic data from offspring to identify interactions. These studies are underway. It will be interesting to compare the metabolomes of the exposed mother and F1 and F2 generations which were not directly exposed to BTP to confirm if the effects of biosolids exposure on the metabolome is transient or persistent.

This study brings to light the importance of understanding how environmental chemicals may cause adverse outcomes. Our findings raise a question on the widespread use of biosolids as alternative to inorganic chemical fertilizers, which can be problematic at two levels: 1) it introduces a cocktail of environmental chemicals, including endocrine disruptors, into the ecosystem that ultimately constitutes our food chain, with the potential risk of biomagnification, and 2) consuming food, from either plant or animal sources, contaminated with environmental chemicals amplifies our daily exposure to these chemicals and exposes us to a new array of chemicals. This raises the question if switching to biosolid fertilizers over conventional chemical fertilizers is as beneficial as originally believed.

5. Conclusion:

Our study provides evidence that exposure to biosolids significantly alters the maternal metabolome, which is characterized by changes in lipid and branched chain amino acid metabolism, possibly as a response to oxidative stress from the exposure to chemicals present in the biosolids. These factors likely contribute to the adverse metabolic outcomes observed previously in the offspring. Biosolids exposure represents real-life, day-to-day exposure to chemicals, including endocrine disruptors. This is the first study to show that a real-life scenario of chemical exposure can influence whole body metabolism, which could have major consequences in both adults and pregnant mothers.

Acknowledgements: We thank Dr. Nadia Saadat, Research Investigator, Department of Pediatrics-Endocrinology, University of Michigan, for her inputs on the bioinformatics analyses.

References :

1. Gore AC, Chappell VA, Fenton SE, et al. EDC-2: The Endocrine Society's Second Scientific Statement on Endocrine-Disrupting Chemicals. *Endocrine Reviews*. 2015/12// 2015;36(6):E1-E150. doi:10.1210/ER.2015-1010
2. Kumar M, Sarma DK, Shubham S, et al. Environmental Endocrine-Disrupting Chemical Exposure: Role in Non-Communicable Diseases. *Front Public Health*. 2020;8:553850. doi:10.3389/fpubh.2020.553850
3. Heindel JJ, Blumberg B, Cave M, et al. Metabolism disrupting chemicals and metabolic disorders. *Reprod Toxicol*. Mar 2017;68:3-33. doi:10.1016/j.reprotox.2016.10.001
4. Nicolella HD, de Assis S. Epigenetic Inheritance: Intergenerational Effects of Pesticides and Other Endocrine Disruptors on Cancer Development. *Int J Mol Sci*. Apr 23 2022;23(9)doi:10.3390/ijms23094671
5. Attina TM, Hauser R, Sathyanarayana S, et al. Exposure to endocrine-disrupting chemicals in the USA: a population-based disease burden and cost analysis. *The lancet Diabetes & endocrinology*. 2016/12// 2016;4(12):996-1003. doi:10.1016/S2213-8587(16)30275-3
6. Harper AP, Finger BJ, Green MP. Chronic Atrazine Exposure Beginning Prenatally Impacts Liver Function and Sperm Concentration With Multi-Generational Consequences in Mice. *Frontiers in endocrinology*. 2020/11// 2020;11doi:10.3389/FENDO.2020.580124
7. Gingrich J, Pu Y, Roberts J, et al. Gestational bisphenol S impairs placental endocrine function and the fusogenic trophoblast signaling pathway. *Archives of toxicology*. 2018/5// 2018;92(5):1861-1876. doi:10.1007/S00204-018-2191-2
8. Rodprasert W, Toppari J, Virtanen HE. Endocrine Disrupting Chemicals and Reproductive Health in Boys and Men. *Front Endocrinol (Lausanne)*. 2021;12:706532. doi:10.3389/fendo.2021.706532
9. Turan S. Endocrine disrupting chemicals and bone. *Best Pract Res Clin Endocrinol Metab*. Sep 2021;35(5):101495. doi:10.1016/j.beem.2021.101495
10. López-Rodríguez D, Aylwin CF, Delli V, et al. Multi- and Transgenerational Outcomes of an Exposure to a Mixture of Endocrine-Disrupting Chemicals (EDCs) on Puberty and Maternal Behavior in the Female Rat. *Environmental Health Perspectives*. 2021/8// 2021;129(8)doi:10.1289/EHP8795
11. Caporale N, Leemans M, Birgersson L, et al. From cohorts to molecules: Adverse impacts of endocrine disrupting mixtures. *Science*. 2022/2// 2022;375(6582)doi:10.1126/SCIENCE.ABE8244/SUPPL_FILE/SCIENCE.ABE8244_MDAR_REPRODUCIBILITY_CHECKLIST.PDF
12. Elcombe CS, Evans NP, Bellingham M. Critical review and analysis of literature on low dose exposure to chemical mixtures in mammalian in vivo systems. *Crit Rev Toxicol*. Mar 2022;52(3):221-238. doi:10.1080/10408444.2022.2091423

13. Ketema RM, Ait Bamai Y, Miyashita C, Saito T, Kishi R, Ikeda-Araki A. Phthalates mixture on allergies and oxidative stress biomarkers among children: The Hokkaido study. *Environment International*. 2022/2// 2022;160:107083-107083. doi:10.1016/J.ENVINT.2022.107083
14. Wu M, Shu Y, Wang Y. Exposure to mixture of heavy metals and muscle strength in children and adolescents: a population-based study. *Environmental Science and Pollution Research 2022*. 2022/4// 2022;1:1-9. doi:10.1007/S11356-022-19916-2
15. Roth K, Yang Z, Agarwal M, et al. Exposure to a mixture of legacy, alternative, and replacement per- and polyfluoroalkyl substances (PFAS) results in sex-dependent modulation of cholesterol metabolism and liver injury. *Environment International*. 2021/12// 2021;157:106843-106843. doi:10.1016/J.ENVINT.2021.106843
16. Kelley AS, Banker M, Goodrich JM, et al. Early pregnancy exposure to endocrine disrupting chemical mixtures are associated with inflammatory changes in maternal and neonatal circulation. *Sci Rep*. Apr 1 2019;9(1):5422. doi:10.1038/s41598-019-41134-z
17. Pearce JL, Neelon B, Bloom MS, et al. Exploring associations between prenatal exposure to multiple endocrine disruptors and birth weight with exposure continuum mapping. *Environmental Research*. 2021/9// 2021;200:111386-111386. doi:10.1016/J.ENVRES.2021.111386
18. Gore AC, Moore T, Groom MJ, Thompson LM. Prenatal Exposure to an EDC Mixture, NeuroMix: Effects on Brain, Behavior, and Stress Responsiveness in Rats. *Toxics 2022, Vol 10, Page 122*. 2022/3// 2022;10(3):122-122. doi:10.3390/TOXICS10030122
19. Hu JMY, Arbuckle TE, Janssen P, et al. Prenatal exposure to endocrine disrupting chemical mixtures and infant birth weight: A Bayesian analysis using kernel machine regression. *Environmental research*. 2021/4// 2021;195doi:10.1016/J.ENVRES.2021.110749
20. Schüttler A, Jakobs G, Fix JM, et al. Transcriptome-Wide Prediction and Measurement of Combined Effects Induced by Chemical Mixture Exposure in Zebrafish Embryos. *Environmental Health Perspectives*. 2021/4// 2021;129(4)doi:10.1289/EHP7773
21. Kortenkamp A, Scholze M, Ermler S, et al. Combined exposures to bisphenols, polychlorinated dioxins, paracetamol, and phthalates as drivers of deteriorating semen quality. *Environ Int*. Jul 2022;165:107322. doi:10.1016/j.envint.2022.107322
22. Ribeiro E, Ladeira C, Viegas S. EDCs Mixtures: A Stealthy Hazard for Human Health? *Toxics*. 2017/3// 2017;5(1)doi:10.3390/TOXICS5010005
23. Rodea-Palomares I, Gonzalez-Pleiter M, Gonzalo S, et al. Hidden drivers of low-dose pharmaceutical pollutant mixtures revealed by the novel GSA-QHTS screening method. *Science Advances*. 2016/9// 2016;2(9)doi:10.1126/SCIADV.1601272/SUPPL_FILE/1601272_SM.PDF
24. USEPA. Biosolids Annual Program Reports 2019 | United States Environmental Protection Agency. United States Environmental Protection Agency. Washington,DC: United States Environmental Protection Agency; 2019.
25. Harley-Nyang D, Memon FA, Jones N, Galloway T. Investigation and analysis of microplastics in sewage sludge and biosolids: A case study from one wastewater treatment works in the UK. *Science of The Total Environment*. 2022/6// 2022;823:153735-153735. doi:10.1016/J.SCITOTENV.2022.153735
26. Smith SR. Organic contaminants in sewage sludge (biosolids) and their significance for agricultural recycling. *Trans R Soc A*. 2009;367:4005-4041. doi:10.1098/rsta.2009.0154
27. Moodie D, Coggan T, Berry K, et al. Legacy and emerging per- and polyfluoroalkyl substances (PFASs) in Australian biosolids. *Chemosphere*. 2021/5// 2021;270:129143-129143. doi:10.1016/J.CHEMOSPHERE.2020.129143

28. Rhind SM, Smith A, Kyle CE, et al. Phthalate and alkyl phenol concentrations in soil following applications of inorganic fertiliser or sewage sludge to pasture and potential rates of ingestion by grazing ruminants. *J Environ Monit*. Feb 2002;4(1):142-8. doi:10.1039/b107539j
29. Zhang Z, Le Velly M, Rhind SM, et al. A study on temporal trends and estimates of fate of Bisphenol A in agricultural soils after sewage sludge amendment. *Sci Total Environ*. May 15 2015;515-516:1-11. doi:10.1016/j.scitotenv.2015.01.053
30. Komesli OT, Muz M, Ak MS, Bakirdere S, Gokcay CF. Occurrence, fate and removal of endocrine disrupting compounds (EDCs) in Turkish wastewater treatment plants. *Chemical Engineering Journal*. 2015/10// 2015;277:202-208. doi:10.1016/J.CEJ.2015.04.115
31. Evans NP, Bellingham M, Sharpe RM, et al. Reproduction Symposium: does grazing on biosolids-treated pasture pose a pathophysiological risk associated with increased exposure to endocrine disrupting compounds? *J Anim Sci*. 2014;92(8)(1525-3163 (Electronic)):3185-98. doi:doi: 10.2527/jas.2014-7763
32. Venkatesan AK, Halden RU. Contribution of polybrominated dibenzo-p-dioxins and dibenzofurans (PBDD/Fs) to the toxic equivalency of dioxin-like compounds in archived biosolids from the U.S. EPA's 2001 national sewage sludge survey. *Environ Sci Technol*. Sep 16 2014;48(18):10843-9. doi:10.1021/es503110j
33. Cavanagh JE, Trought K, Mitchell C, Northcott G, Tremblay LA. Assessment of endocrine disruption and oxidative potential of bisphenol-A, triclosan, nonylphenol, diethylhexyl phthalate, galaxolide, and carbamazepine, common contaminants of municipal biosolids. *Toxicol In Vitro*. Apr 2018;48:342-349. doi:10.1016/j.tiv.2018.02.003
34. Rhind SM, Kyle CE, Ruffie H, et al. Short- and long-term temporal changes in soil concentrations of selected endocrine disrupting compounds (EDCs) following single or multiple applications of sewage sludge to pastures. *Environ Pollut*. Oct 2013;181:262-70. doi:10.1016/j.envpol.2013.06.011
35. Rhind SM, Kyle CE, MacKie C, McDonald L. Accumulation of endocrine disrupting compounds in sheep fetal and maternal liver tissue following exposure to pastures treated with sewage sludge. *Journal of Environmental Monitoring*. 2009/8// 2009;11(8):1469-1476. doi:10.1039/B902085C
36. Rhind SM, Kyle CE, Mackie C, et al. Maternal and fetal tissue accumulation of selected endocrine disrupting compounds (EDCs) following exposure to sewage sludge-treated pastures before or after conception. *J Environ Monit*. Aug 5 2010;12(8):1582-93. doi:10.1039/c0em00009d
37. Morrison JL, Berry MJ, Botting KJ, et al. Improving pregnancy outcomes in humans through studies in sheep. *Am J Physiol Regul Integr Comp Physiol*. Dec 1 2018;315(6):R1123-R1153. doi:10.1152/ajpregu.00391.2017
38. Padmanabhan V, Veiga-Lopez A. Sheep models of polycystic ovary syndrome phenotype. *Mol Cell Endocrinol*. Jul 5 2013;373(1-2):8-20. doi:10.1016/j.mce.2012.10.005
39. Wu C, Spongberg AL, Witter JD, Sridhar BB. Transfer of wastewater associated pharmaceuticals and personal care products to crop plants from biosolids treated soil. *Ecotoxicol Environ Saf*. Nov 2012;85:104-9. doi:10.1016/j.ecoenv.2012.08.007
40. Jedynak P, Tost J, Calafat AM, et al. Pregnancy exposure to phthalates and DNA methylation in male placenta — An epigenome-wide association study. *Environment International*. 2022/2// 2022;160:107054-107054. doi:10.1016/J.ENVINT.2021.107054
41. Elcombe CS, Monteiro A, Ghasemzadeh-Hasankolaei M, Evans NP, Bellingham M. Morphological and transcriptomic alterations in neonatal lamb testes following developmental

exposure to low-level environmental chemical mixture. *Environmental Toxicology and Pharmacology*. 2021/8// 2021;86:103670-103670. doi:10.1016/J.ETAP.2021.103670
42. Lea RG, Mandon-Pépin B, Loup B, et al. Ovine fetal testis stage-specific sensitivity to environmental chemical mixtures. *Reproduction*. 2022/2// 2022;163(2):119-131. doi:10.1530/REP-21-0235
43. Chang CH, Tsai YA, Huang YF, et al. The sex-specific association of prenatal phthalate exposure with low birth weight and small for gestational age: A nationwide survey by the Taiwan Maternal and Infant Cohort Study (TMICS). *Science of The Total Environment*. 2022/2// 2022;806:151261-151261. doi:10.1016/J.SCITOTENV.2021.151261
44. Puttabyatappa M, Sargis RM, Padmanabhan V. Developmental programming of insulin resistance: are androgens the culprits? *J Endocrinol*. Jun 2020;245(3):R23-R48. doi:10.1530/JOE-20-0044
45. Song W, Puttabyatappa M, Zeng L, Vazquez D, Pennathur S, Padmanabhan V. Developmental programming: Prenatal bisphenol A treatment disrupts mediators of placental function in sheep. *Chemosphere*. Mar 2020;243:125301. doi:10.1016/j.chemosphere.2019.125301
46. Vyas AK, Hoang V, Padmanabhan V, Gilbreath E, Mietelka KA. Prenatal programming: adverse cardiac programming by gestational testosterone excess. *Sci Rep*. Jun 22 2016;6:28335. doi:10.1038/srep28335
47. Bellingham M, Fowler PA, MacDonald ES, et al. Timing of Maternal Exposure and Foetal Sex Determine the Effects of Low-level Chemical Mixture Exposure on the Foetal Neuroendocrine System in Sheep. *J Neuroendocrinol*. Dec 2016;28(12)doi:10.1111/jne.12444
48. Rahman F, Coull BA, Carroll KN, et al. Prenatal PM2.5 exposure and infant temperament at age 6 months: Sensitive windows and sex-specific associations. *Environmental Research*. 2022/4// 2022;206:112583-112583. doi:10.1016/J.ENVRES.2021.112583
49. Lind PM, Oberg D, Larsson S, Kyle CE, Orberg J, Rhind SM. Pregnant ewes exposed to multiple endocrine disrupting pollutants through sewage sludge-fertilized pasture show an anti-estrogenic effect in their trabecular bone. *Sci Total Environ*. May 1 2010;408(11):2340-6. doi:10.1016/j.scitotenv.2010.01.059
50. Bellingham M, Fowler PA, Amezaga MR, et al. Exposure to a complex cocktail of environmental endocrine-disrupting compounds disturbs the kisspeptin/GPR54 system in ovine hypothalamus and pituitary gland. *Environmental health perspectives*. 2009/10// 2009;117(10):1556-1562. doi:10.1289/EHP.0900699
51. Bellingham M, Fowler PA, Amezaga MR, et al. Foetal hypothalamic and pituitary expression of gonadotrophin-releasing hormone and galanin systems is disturbed by exposure to sewage sludge chemicals via maternal ingestion. *Journal of neuroendocrinology*. 2010;22(6):527-533. doi:10.1111/J.1365-2826.2010.01974.X
52. Bellingham M, McKinnell C, Fowler PA, et al. Foetal and post-natal exposure of sheep to sewage sludge chemicals disrupts sperm production in adulthood in a subset of animals. *International Journal of Andrology*. 2012;35(3):317-329. doi:10.1111/j.1365-2605.2011.01234.x
53. Elcombe CS, Monteiro A, Elcombe MR, Ghasemzadeh-Hasankolaei M, Evans NP, Bellingham M. Testicular Dysgenesis Syndrome-like morphology and gene expression, and activation of Hypoxia Inducible Factor 1 Alpha in juvenile lamb testes following developmental exposure to low-level environmental chemical mixture. *bioRxiv*. 2022/2// 2022:2022.02.08.479595-2022.02.08.479595. doi:10.1101/2022.02.08.479595

54. Paul C, Rhind SM, Kyle CE, Scott H, McKinnell C, Sharpe RM. Cellular and hormonal disruption of fetal testis development in sheep reared on pasture treated with sewage sludge. *Environ Health Perspect*. Nov 2005;113(11):1580-7. doi:10.1289/ehp.8028
55. Bellingham M, Amezaga MR, Mandon-Pepin B, et al. Exposure to chemical cocktails before or after conception--- the effect of timing on ovarian development. *Molecular and cellular endocrinology*. 2013/8// 2013;376(1-2):156-172. doi:10.1016/J.MCE.2013.06.016
56. Fowler PA, Dorà NJ, McFerran H, et al. In utero exposure to low doses of environmental pollutants disrupts fetal ovarian development in sheep. *Molecular human reproduction*. 2008/5// 2008;14(5):269-280. doi:10.1093/MOLEHR/GAN020
57. Hombach-Klonisch S, Danescu A, Begum F, et al. Peri-conceptional changes in maternal exposure to sewage sludge chemicals disturbs fetal thyroid gland development in sheep. *Mol Cell Endocrinol*. Mar 10 2013;367(1-2):98-108. doi:10.1016/j.mce.2012.12.022
58. Kadakia R, Nodzenski M, Talbot O, et al. Maternal metabolites during pregnancy are associated with newborn outcomes and hyperinsulinaemia across ancestries. *Diabetologia*. 2019/3// 2019;62(3):473-484. doi:10.1007/S00125-018-4781-1/FIGURES/7
59. Lesseur C, Chen J. Adverse Maternal Metabolic Intrauterine Environment and Placental Epigenetics: Implications for Fetal Metabolic Programming. *Current environmental health reports*. 2018/12// 2018;5(4):531-543. doi:10.1007/S40572-018-0217-9/FIGURES/1
60. Bowman CE, Arany Z, Wolfgang MJ. Regulation of maternal–fetal metabolic communication. *Cellular and Molecular Life Sciences 2020 78:4*. 2020/10// 2020;78(4):1455-1486. doi:10.1007/S00018-020-03674-W
61. Petrick LM, Uppal K, Funk WE. Metabolomics and adductomics of newborn bloodspots to retrospectively assess the early-life exposome. *Current opinion in pediatrics*. 2020/4// 2020;32(2):300-300. doi:10.1097/MOP.0000000000000875
62. Cai Y, Rosen Vollmar AK, Johnson CH. Analyzing Metabolomics Data for Environmental Health and Exposome Research. *Methods in Molecular Biology*. 2020;2104:447-467. doi:10.1007/978-1-0716-0239-3_22
63. Chen Y, Guo J, Xing S, Yu H, Huan T. Global-Scale Metabolomic Profiling of Human Hair for Simultaneous Monitoring of Endogenous Metabolome, Short- and Long-Term Exposome. *Frontiers in Chemistry*. 2021/5// 2021;9:281-281. doi:10.3389/FCHEM.2021.674265/BIBTEX
64. Chamorro-García R, Poupin N, Tremblay-Franco M, et al. Transgenerational metabolomic fingerprints in mice ancestrally exposed to the obesogen TBT. *Environment International*. 2021/12// 2021;157:106822-106822. doi:10.1016/J.ENVINT.2021.106822
65. Zhao H, Liu M, Lv Y, Fang M. Dose-response metabolomics and pathway sensitivity to map molecular cartography of bisphenol A exposure. *Environment International*. 2022/1// 2022;158:106893-106893. doi:10.1016/J.ENVINT.2021.106893
66. Sun J, Fang R, Wang H, et al. A review of environmental metabolism disrupting chemicals and effect biomarkers associating disease risks: Where exposomics meets metabolomics. *Environ Int*. Jan 2022;158:106941. doi:10.1016/j.envint.2021.106941
67. Kachman M, Habra H, Duren W, et al. Deep annotation of untargeted LC-MS metabolomics data with Binner. *Bioinformatics*. Mar 1 2020;36(6):1801-1806. doi:10.1093/bioinformatics/btz798
68. Dunn WB, Broadhurst D, Begley P, et al. Procedures for large-scale metabolic profiling of serum and plasma using gas chromatography and liquid chromatography coupled to mass spectrometry. *Nat Protoc*. Jun 30 2011;6(7):1060-83. doi:10.1038/nprot.2011.335

69. Sumner LW, Amberg A, Barrett D, et al. Proposed minimum reporting standards for chemical analysis Chemical Analysis Working Group (CAWG) Metabolomics Standards Initiative (MSI). *Metabolomics : Official journal of the Metabolomic Society*. 2007/9// 2007;3(3):211-211. doi:10.1007/S11306-007-0082-2
70. Faquih T, van Smeden M, Luo J, et al. A Workflow for Missing Values Imputation of Untargeted Metabolomics Data. *Metabolites*. Nov 26 2020;10(12)doi:10.3390/metabo10120486
71. Schiffman C, Petrick L, Perttula K, et al. Filtering procedures for untargeted LC-MS metabolomics data. *BMC Bioinformatics*. Jun 14 2019;20(1):334. doi:10.1186/s12859-019-2871-9
72. Wilson MD, Ponzini MD, Taylor SL, Kim K. Imputation of Missing Values for Multi-Biospecimen Metabolomics Studies: Bias and Effects on Statistical Validity. *Metabolites*. Jul 21 2022;12(7)doi:10.3390/metabo12070671
73. van den Berg RA, Hoefsloot HCJ, Westerhuis JA, Smilde AK, van der Werf MJ. Centering, scaling, and transformations: Improving the biological information content of metabolomics data. *BMC Genomics*. 2006/6// 2006;7(1):1-15. doi:10.1186/1471-2164-7-142/FIGURES/9
74. Worley B, Powers R. PCA as a practical indicator of OPLS-DA model reliability. *Curr Metabolomics*. 2016;4(2):97-103. doi:10.2174/2213235X04666160613122429
75. Qu R, Xie Q, Tian J, Zhou M, Ge F. Metabolomics reveals the inhibition on phosphorus assimilation in Chlorella vulgaris F1068 exposed to AgNPs. *Sci Total Environ*. May 20 2021;770:145362. doi:10.1016/j.scitotenv.2021.145362
76. Zhao C, Ge J, Li X, et al. Integrated metabolome analysis reveals novel connections between maternal fecal metabolome and the neonatal blood metabolome in women with gestational diabetes mellitus. *Sci Rep*. Feb 27 2020;10(1):3660. doi:10.1038/s41598-020-60540-2
77. Westerhuis JA, van Velzen EJJ, Hoefsloot HCJ, Smilde AK. Discriminant Q2 (DQ2) for improved discrimination in PLSDA models. *Metabolomics*. 2008/8// 2008;4(4):293-296. doi:10.1007/S11306-008-0126-2/FIGURES/3
78. Eriksson L, Kettaneh-Wold N, Trygg J, Wikström C, Wold S. *Multi- and Megavariate Data Analysis : Part I: Basic Principles and Applications*. Umetrics Inc; 2006:425.
79. Saccenti E, Hoefsloot HCJ, Smilde AK, Westerhuis JA, Hendriks MMWB. Reflections on univariate and multivariate analysis of metabolomics data. *Metabolomics*. 2014/06/01 2014;10(3):361-374. doi:10.1007/s11306-013-0598-6
80. Schaefer-Graf UM, Graf K, Kulbacka I, et al. Maternal lipids as strong determinants of fetal environment and growth in pregnancies with gestational diabetes mellitus. *Diabetes Care*. Sep 2008;31(9):1858-63. doi:10.2337/dc08-0039
81. Gootjes DV, Posthumus AG, Wols DF, de Rijke YB, Roeters Van Lennep JE, Steegers EAP. Maternal lipid profile in pregnancy and embryonic size: a population-based prospective cohort study. *BMC Pregnancy Childbirth*. Apr 18 2022;22(1):333. doi:10.1186/s12884-022-04647-6
82. Duttaroy AK, Basak S. Maternal Fatty Acid Metabolism in Pregnancy and Its Consequences in the Feto-Placental Development. *Front Physiol*. 2021;12:787848. doi:10.3389/fphys.2021.787848
83. Kabaran S, Besler HT. Do fatty acids affect fetal programming? *J Health Popul Nutr*. Aug 13 2015;33:14. doi:10.1186/s41043-015-0018-9
84. Delhaes F, Giza SA, Koreman T, et al. Altered maternal and placental lipid metabolism and fetal fat development in obesity: Current knowledge and advances in non-invasive assessment. *Placenta*. Sep 2018;69:118-124. doi:10.1016/j.placenta.2018.05.011

85. Dunning KR, Russell DL, Robker RL. Lipids and oocyte developmental competence: the role of fatty acids and beta-oxidation. *Reproduction*. Jul 2014;148(1):R15-27. doi:10.1530/REP-13-0251
86. Collodel G, Moretti E, Noto D, Iacoponi F, Signorini C. Fatty Acid Profile and Metabolism Are Related to Human Sperm Parameters and Are Relevant in Idiopathic Infertility and Varicocele. *Mediators Inflamm*. 2020;2020:3640450. doi:10.1155/2020/3640450
87. Longo N, Frigeni M, Pasquali M. Carnitine transport and fatty acid oxidation. *Biochim Biophys Acta*. Oct 2016;1863(10):2422-35. doi:10.1016/j.bbamcr.2016.01.023
88. Elshenawy S, Pinney SE, Stuart T, et al. The Metabolomic Signature of the Placenta in Spontaneous Preterm Birth. *Int J Mol Sci*. Feb 4 2020;21(3)doi:10.3390/ijms21031043
89. Shekhawat P, Bennett MJ, Sadovsky Y, Nelson DM, Rakheja D, Strauss AW. Human placenta metabolizes fatty acids: implications for fetal fatty acid oxidation disorders and maternal liver diseases. *Am J Physiol Endocrinol Metab*. Jun 2003;284(6):E1098-105. doi:10.1152/ajpendo.00481.2002
90. Hiley CR, Hoi PM. Oleamide: A Fatty Acid Amide Signaling Molecule in the Cardiovascular System? *Cardiovascular Drug Reviews*. 2007/3// 2007;25(1):46-60. doi:10.1111/J.1527-3466.2007.00004.X
91. Valerio E, Mardegan V, Stocchero M, et al. Urinary metabotypes of newborns with perinatal asphyxia undergoing therapeutic hypothermia. *PLoS One*. 2022;17(8):e0273175. doi:10.1371/journal.pone.0273175
92. Cui Y, Liu X, Wang M, et al. Lysophosphatidylcholine and amide as metabolites for detecting alzheimer disease using ultrahigh-performance liquid chromatography-quadrupole time-of-flight mass spectrometry-based metabonomics. *J Neuropathol Exp Neurol*. Oct 2014;73(10):954-63. doi:10.1097/NEN.0000000000000116
93. Leggett JD, Aspley S, Beckett SR, D'Antona AM, Kendall DA, Kendall DA. Oleamide is a selective endogenous agonist of rat and human CB1 cannabinoid receptors. *Br J Pharmacol*. Jan 2004;141(2):253-62. doi:10.1038/sj.bjp.0705607
94. Ezechukwu HC, Diya CA, Shrestha N, Hryciw DH. Role for endocannabinoids in early pregnancy: recent advances and the effects of cannabis use. *Am J Physiol Endocrinol Metab*. Sep 1 2020;319(3):E557-E561. doi:10.1152/ajpendo.00210.2020
95. De Domenico E, Todaro F, Rossi G, et al. Overactive type 2 cannabinoid receptor induces meiosis in fetal gonads and impairs ovarian reserve. *Cell Death Dis*. Oct 5 2017;8(10):e3085. doi:10.1038/cddis.2017.496
96. Lopez-Cardona AP, Perez-Cerezales S, Fernandez-Gonzalez R, et al. CB1 cannabinoid receptor drives oocyte maturation and embryo development via PI3K/Akt and MAPK pathways. *FASEB J*. Aug 2017;31(8):3372-3382. doi:10.1096/fj.201601382RR
97. Tam J, Ofek O, Fride E, et al. Involvement of neuronal cannabinoid receptor CB1 in regulation of bone mass and bone remodeling. *Mol Pharmacol*. Sep 2006;70(3):786-92. doi:10.1124/mol.106.026435
98. Hillard CJ. Endocannabinoids and the Endocrine System in Health and Disease. *Handb Exp Pharmacol*. 2015;231:317-39. doi:10.1007/978-3-319-20825-1_11
99. Nielsen JE, Rolland AD, Rajpert-De Meyts E, et al. Characterisation and localisation of the endocannabinoid system components in the adult human testis. *Sci Rep*. Sep 19 2019;9(1):12866. doi:10.1038/s41598-019-49177-y
100. Dowhan W. Synthesis and Structure of Glycerolipids. In: Bradshaw RA, Stahl PD, eds. *Encyclopedia of Cell Biology*. Academic Press; 2016:160-172.

101. Tindula G, Lee D, Huen K, Bradman A, Eskenazi B, Holland N. Pregnancy lipidomic profiles and DNA methylation in newborns from the CHAMACOS cohort. *Environ Epigenet*. Jan 2019;5(1):dvz004. doi:10.1093/eep/dvz004
102. Bartke N, Hannun YA. Bioactive sphingolipids: metabolism and function. *J Lipid Res*. Apr 2009;50 Suppl:S91-6. doi:10.1194/jlr.R800080-JLR200
103. Qi T, Li L, Weidong T. The Role of Sphingolipid Metabolism in Bone Remodeling. *Front Cell Dev Biol*. 2021;9:752540. doi:10.3389/fcell.2021.752540
104. Dai Y, Huo X, Cheng Z, Faas MM, Xu X. Early-life exposure to widespread environmental toxicants and maternal-fetal health risk: A focus on metabolomic biomarkers. *Sci Total Environ*. Oct 15 2020;739:139626. doi:10.1016/j.scitotenv.2020.139626
105. Guo X, Zhang L, Wang J, et al. Plasma metabolomics study reveals the critical metabolic signatures for benzene-induced hematotoxicity. *JCI Insight*. Jan 25 2022;7(2)doi:10.1172/jci.insight.154999
106. Kerzic PJ, Liu WS, Pan MT, et al. Analysis of hydroquinone and catechol in peripheral blood of benzene-exposed workers. *Chem Biol Interact*. Mar 19 2010;184(1-2):182-8. doi:10.1016/j.cbi.2009.12.010
107. Sun R, Cao M, Zhang J, et al. Benzene Exposure Alters Expression of Enzymes Involved in Fatty Acid beta-Oxidation in Male C3H/He Mice. *Int J Environ Res Public Health*. Oct 31 2016;13(11)doi:10.3390/ijerph13111068
108. Rice GM, Steiner RD. Inborn Errors of Metabolism (Metabolic Disorders). *Pediatr Rev*. Jan 2016;37(1):3-15; quiz 16-7, 47. doi:10.1542/pir.2014-0122
109. Jones PM, Bennett MJ. Disorders of mitochondrial fatty acid β-oxidation. *Biomarkers in Inborn Errors of Metabolism*. 2017:87-101. doi:10.1016/B978-0-12-802896-4.00005-5
110. Zhang Y, Li F, Patterson AD, et al. Abcb11 deficiency induces cholestasis coupled to impaired beta-fatty acid oxidation in mice. *J Biol Chem*. Jul 13 2012;287(29):24784-94. doi:10.1074/jbc.M111.329318
111. Rucker RB, Morris J, Fascetti AJ. Vitamins. *Clinical Biochemistry of Domestic Animals*. 2008:695-730. doi:10.1016/B978-0-12-370491-7.00023-4
112. Baker H, Thind IS, Frank O, DeAngelis B, Caterini H, Louria DB. Vitamin levels in low-birth-weight newborn infants and their mothers. *Am J Obstet Gynecol*. Nov 1 1977;129(5):521-4. doi:10.1016/0002-9378(77)90090-4
113. Wu G, Bazer FW, Dai Z, Li D, Wang J, Wu Z. Amino Acid Nutrition in Animals: Protein Synthesis and Beyond. *Annual Review of Animal Biosciences*. 2014;2(1):387-417. doi:10.1146/annurev-animal-022513-114113
114. Zaitsu K, Asano T, Kawakami D, et al. Metabolomics and Data-Driven Bioinformatics Revealed Key Maternal Metabolites Related to Fetal Lethality via Di(2-ethylhexyl)phthalate Exposure in Pregnant Mice. *ACS Omega*. 2022;7(27):23717-23726. doi:10.1021/acsomega.2c02338
115. Lea RG, Amezaga MR, Loup B, et al. The fetal ovary exhibits temporal sensitivity to a 'real-life' mixture of environmental chemicals. *Scientific Reports*. 2016;6(February):1-13. doi:10.1038/srep22279
116. Chetla VS, Bommu S, Laxmi NA, Putty K, Reddy KK, Bharani KK. Comparative evaluation of the effect of L-Arginine and L-Homoarginine supplementation on reproductive physiology in ewes. *Research in Veterinary Science*. 2022;149:159-171. doi:10.1016/j.rvsc.2022.06.022
117. Wu G. Amino acids: Metabolism, functions, and nutrition. *Amino Acids*. 2009;37(1):1-17. doi:10.1007/s00726-009-0269-0

118. Paul C, Rhind SM, Kyle CE, Scott H, McKinnell C, Sharpe RM. Cellular and Hormonal Disruption of Fetal Testis Development in Sheep Reared on Pasture Treated with Sewage Sludge. *Environmental Health Perspectives*. 2005;113(11):1580-1587. doi:10.1289/ehp.8028
119. Bélanger R, Chandramohan N, Misbin R, Rivlin RS. Tyrosine and glutamic acid in plasma and urine of patients with altered thyroid function. *Metabolism*. 1972;21(9):855-865. doi:10.1016/0026-0495(72)90009-1
120. Field MS, Kamynina E, Stover PJ. MTHFD1 regulates nuclear de novo thymidylate biosynthesis and genome stability. *Biochimie*. 2016;126:27-30. doi:10.1016/j.biochi.2016.02.001
121. Anderson OS, Sant KE, Dolinoy DC. Nutrition and epigenetics: an interplay of dietary methyl donors, one-carbon metabolism and DNA methylation. *The Journal of Nutritional Biochemistry*. 2012;23(8):853-859. doi:10.1016/j.jnutbio.2012.03.003
122. Clare CE, Brassington AH, Kwong WY, Sinclair KD. One-Carbon Metabolism: Linking Nutritional Biochemistry to Epigenetic Programming of Long-Term Development. *Annu Rev Anim Biosci*. Feb 15 2019;7:263-287. doi:10.1146/annurev-animal-020518-115206
123. Kwon H, Spencer TE, Bazer FW, Wu G. Developmental changes of amino acids in ovine fetal fluids. *Biology of Reproduction*. 2003;68(5):1813-1820. doi:10.1095/biolreprod.102.012971
124. Cui Z, Feng H, He B, He J, Tian Y. Relationship Between Serum Amino Acid Levels and Bone Mineral Density: A Mendelian Randomization Study. *Frontiers in Endocrinology*. 2021;9(12):763638-763638. doi:10.3389/fendo.2021.763538
125. White PJ, Lapworth AL, An J, et al. Branched-chain amino acid restriction in Zucker-fatty rats improves muscle insulin sensitivity by enhancing efficiency of fatty acid oxidation and acyl-glycine export. *Molecular Metabolism*. 2016;5(7):538-551. doi:10.1016/j.molmet.2016.04.006
126. Clare CE, Brassington AH, Kwong WY, Sinclair KD. One-Carbon Metabolism: Linking Nutritional Biochemistry to Epigenetic Programming of Long-Term Development. *Annual Review of Animal Biosciences*. 2019;7(1):263-287. doi:10.1146/annurev-animal-020518-115206
127. Nie C, He T, Zhang W, Zhang G, Ma X. Branched Chain Amino Acids: Beyond Nutrition Metabolism. *International Journal of Molecular Sciences*. 2018;19(4):954-954. doi:10.3390/ijms19040954
128. Nemutlu E, Orgul G, Recber T, et al. Metabolic Infrastructure of Pregnant Women With Trisomy 21 Fetuses; Metabolomic Analysis. *Z Geburtshilfe Neonatol*. Oct 2019;223(5):297-303. doi:10.1055/a-0877-7869
129. Ziboh VA. The significance of polyunsaturated fatty acids in cutaneous biology. *Lipids*. Mar 1996;31 Suppl:S249-53. doi:10.1007/BF02637085
130. Vang K, Ziboh VA. 15-lipoxygenase metabolites of gamma-linolenic acid/eicosapentaenoic acid suppress growth and arachidonic acid metabolism in human prostatic adenocarcinoma cells: possible implications of dietary fatty acids. *Prostaglandins Leukot Essent Fatty Acids*. May 2005;72(5):363-72. doi:10.1016/j.plefa.2005.02.002
131. Gaytan-Pacheco N, Lima-Rogel V, Mendez-Mancilla A, et al. Changes in PPAR-gamma Expression Are Associated with microRNA Profiles during Fetal Programming due to Maternal Overweight and Obesity. *Gynecol Obstet Invest*. 2021;86(5):415-426. doi:10.1159/000517116
132. Sheen JM, Yu HR, Tiao MM, et al. Prenatal dexamethasone-induced programmed hypertension and renal programming. *Life Sci*. Jul 1 2015;132:41-8. doi:10.1016/j.lfs.2015.04.005

133. Maniscalco M, Fuschillo S, Paris D, Cutignano A, Sanduzzi A, Motta A. Chapter Five - Clinical metabolomics of exhaled breath condensate in chronic respiratory diseases. In: Makowski GS, ed. *Advances in Clinical Chemistry*. Elsevier; 2019:121-149.
134. Luderer U, Kavanagh TJ, White CC, Faustman EM. Gonadotropin regulation of glutathione synthesis in the rat ovary☆ ☆This work was supported by the University of California Irvine Center for Occupational and Environmental Health, the NIEHS Center for Ecogenetics and Environmental Health at the University of Washington (1 P30 ES07033-03), the NIEHS Superfund Basic Research Program (1 P42 ES-04696-14001 to T.J.K.), and by US EPA #R-825358–01-0 (to E.F.). *Reproductive Toxicology*. 2001/09/01/ 2001;15(5):495-504. doi:https://doi.org/10.1016/S0890-6238(01)00157-5
135. Zhang D, Li W, Zhang J, et al. Study on urinary metabolic profile of phenylketonuria by micellar electrokinetic capillary chromatography with dual electrochemical detection--potential clinical application in fast diagnosis of phenylketonuria. *Anal Chim Acta*. May 23 2011;694(1-2):61-6. doi:10.1016/j.aca.2011.03.044
136. Schmidt S, Westhoff TH, Krauser P, Zidek W, van der Giet M. The uraemic toxin phenylacetic acid increases the formation of reactive oxygen species in vascular smooth muscle cells. *Nephrol Dial Transplant*. Jan 2008;23(1):65-71. doi:10.1093/ndt/gfm475
137. Bala CG, Rusu A, Ciobanu D, Bucsa C, Roman G. Amino Acid Signature of Oxidative Stress in Patients with Type 2 Diabetes: Targeted Exploratory Metabolomic Research. *Antioxidants (Basel)*. Apr 15 2021;10(4)doi:10.3390/antiox10040610
138. You W, Li HY, Ye LZ, et al. [Screening of biomarkers in exhaled breath of mice exposed to benzene]. *Zhonghua Yu Fang Yi Xue Za Zhi*. May 6 2021;55(5):672-678. doi:10.3760/cma.j.cn112150-20201229-01496
139. Kozlik P, Hasikova L, Stiburkova B, Zavada J, Kalikova K. Rapid and reliable HILIC-MS/MS method for monitoring allantoin as a biomarker of oxidative stress. *Anal Biochem*. Jan 15 2020;589:113509. doi:10.1016/j.ab.2019.113509
140. Zhenyukh O, Civantos E, Ruiz-Ortega M, et al. High concentration of branched-chain amino acids promotes oxidative stress, inflammation and migration of human peripheral blood mononuclear cells via mTORC1 activation. *Free Radic Biol Med*. Mar 2017;104:165-177. doi:10.1016/j.freeradbiomed.2017.01.009
141. McDonagh AF. The biliverdin-bilirubin antioxidant cycle of cellular protection: Missing a wheel? *Free Radic Biol Med*. Sep 1 2010;49(5):814-20. doi:10.1016/j.freeradbiomed.2010.06.001
142. Thomas MM, Haghiac M, Grozav C, Minium J, Calabuig-Navarro V, O'Tierney-Ginn P. Oxidative Stress Impairs Fatty Acid Oxidation and Mitochondrial Function in the Term Placenta. *Reprod Sci*. Jul 2019;26(7):972-978. doi:10.1177/1933719118802054
143. Tonin AM, Ferreira GC, Grings M, et al. Disturbance of mitochondrial energy homeostasis caused by the metabolites accumulating in LCHAD and MTP deficiencies in rat brain. *Life Sci*. May 22 2010;86(21-22):825-31. doi:10.1016/j.lfs.2010.04.003
144. Al-Gubory KH. Environmental pollutants and lifestyle factors induce oxidative stress and poor prenatal development. *Reprod Biomed Online*. Jul 2014;29(1):17-31. doi:10.1016/j.rbmo.2014.03.002
145. Qiao R, Sheng C, Lu Y, Zhang Y, Ren H, Lemos B. Microplastics induce intestinal inflammation, oxidative stress, and disorders of metabolome and microbiome in zebrafish. *Sci Total Environ*. Apr 20 2019;662:246-253. doi:10.1016/j.scitotenv.2019.01.245

146. Puttabyatappa M, Banker M, Zeng L, et al. Maternal Exposure to Environmental Disruptors and Sexually Dimorphic Changes in Maternal and Neonatal Oxidative Stress. *J Clin Endocrinol Metab*. Feb 1 2020;105(2)doi:10.1210/clinem/dgz063
147. Simons GW. The complete subtalar release in clubfeet. *Orthop Clin North Am*. Oct 1987;18(4):667-88.
148. Peters A, Nawrot TS, Baccarelli AA. Hallmarks of environmental insults. *Cell*. Mar 18 2021;184(6):1455-1468. doi:10.1016/j.cell.2021.01.043
149. Prater MR, Laudermilch CL, Liang C, Holladay SD. Placental oxidative stress alters expression of murine osteogenic genes and impairs fetal skeletal formation. *Placenta*. Sep 2008;29(9):802-8. doi:10.1016/j.placenta.2008.06.010
150. Hong Y, Mu X, Ji X, et al. In-utero exposure to HT-2 toxin affects meiotic progression and early oogenesis in foetal oocytes by increasing oxidative stress. *Environ Pollut*. Jun 15 2021;279:116917. doi:10.1016/j.envpol.2021.116917
151. Ghatebi M, Zavareh S, Lashkarbolouki T, Elahdadi Salmani M. Implications from early life stress on the development of mouse ovarian follicles: Focus on oxidative stress. *J Obstet Gynaecol Res*. Aug 2019;45(8):1506-1514. doi:10.1111/jog.14007
152. Yan S, Wang F, Shi Q. The effect of maternal high-fat-diet mediated oxidative stress on ovarian function in mice offspring. *Exp Ther Med*. Dec 2020;20(6):135. doi:10.3892/etm.2020.9264
153. Sobinoff AP, Sutherland JM, Beckett EL, et al. Damaging legacy: maternal cigarette smoking has long-term consequences for male offspring fertility. *Hum Reprod*. Dec 2014;29(12):2719-35. doi:10.1093/humrep/deu235
154. Huang YF, Wang PW, Huang LW, et al. Interactive effects of nonylphenol and bisphenol A exposure with oxidative stress on fetal reproductive indices. *Environ Res*. Nov 2018;167:567-574. doi:10.1016/j.envres.2018.08.007
155. Bolton JL, Auten RL, Bilbo SD. Prenatal air pollution exposure induces sexually dimorphic fetal programming of metabolic and neuroinflammatory outcomes in adult offspring. *Brain Behav Immun*. Mar 2014;37:30-44. doi:10.1016/j.bbi.2013.10.029
156. Gong S, Sovio U, Aye IL, et al. Placental polyamine metabolism differs by fetal sex, fetal growth restriction, and preeclampsia. *JCI Insight*. Jul 12 2018;3(13)doi:10.1172/jci.insight.120723
157. Mitro SD, Wu J, Rahman ML, et al. Longitudinal Plasma Metabolomics Profile in Pregnancy-A Study in an Ethnically Diverse U.S. Pregnancy Cohort. *Nutrients*. Sep 1 2021;13(9)doi:10.3390/nu13093080
158. Woodard V, Thoene M, Van Ormer M, et al. Intrauterine Transfer of Polyunsaturated Fatty Acids in Mother-Infant Dyads as Analyzed at Time of Delivery. *Nutrients*. Mar 19 2021;13(3)doi:10.3390/nu13030996
159. LaBarre JL, Puttabyatappa M, Song PXK, et al. Maternal lipid levels across pregnancy impact the umbilical cord blood lipidome and infant birth weight. *Sci Rep*. Aug 26 2020;10(1):14209. doi:10.1038/s41598-020-71081-z
160. Brass E, Hanson E, O'Tierney-Ginn PF. Placental oleic acid uptake is lower in male offspring of obese women. *Placenta*. Jun 2013;34(6):503-9. doi:10.1016/j.placenta.2013.03.009
161. Powell TL, Barner K, Madi L, et al. Sex-specific responses in placental fatty acid oxidation, esterification and transfer capacity to maternal obesity. *Biochim Biophys Acta Mol Cell Biol Lipids*. Mar 2021;1866(3):158861. doi:10.1016/j.bbalip.2020.158861

162. Geng X, Geng L, Zhang Y, et al. Fetal sex influences maternal fasting plasma glucose levels and basal beta-cell function in pregnant women with normal glucose tolerance. *Acta Diabetol*. Dec 2017;54(12):1131-1138. doi:10.1007/s00592-017-1055-1
163. Giannubilo SR, Pasculli A, Ballatori C, Biagini A, Ciavattini A. Fetal Sex, Need for Insulin, and Perinatal Outcomes in Gestational Diabetes Mellitus: An Observational Cohort Study. *Clin Ther*. Apr 2018;40(4):587-592. doi:10.1016/j.clinthera.2018.02.015
164. Banker M, Puttabyatappa M, O'Day P, et al. Association of Maternal-Neonatal Steroids With Early Pregnancy Endocrine Disrupting Chemicals and Pregnancy Outcomes. *J Clin Endocrinol Metab*. Mar 8 2021;106(3):665-687. doi:10.1210/clinem/dgaa909
165. Cai Y, Rosen Vollmar AK, Johnson CH. Analyzing Metabolomics Data for Environmental Health and Exposome Research. *Methods Mol Biol*. 2020;2104:447-467. doi:10.1007/978-1-0716-0239-3_22
166. Wei S, Wei Y, Gong Y, et al. Metabolomics as a valid analytical technique in environmental exposure research: application and progress. *Metabolomics*. May 31 2022;18(6):35. doi:10.1007/s11306-022-01895-7
167. Deng Y, Zhang Y, Lemos B, Ren H. Tissue accumulation of microplastics in mice and biomarker responses suggest widespread health risks of exposure. *Sci Rep*. Apr 24 2017;7:46687. doi:10.1038/srep46687
168. Li X, Brejnrod AD, Ernst M, et al. Heavy metal exposure causes changes in the metabolic health-associated gut microbiome and metabolites. *Environ Int*. May 2019;126:454-467. doi:10.1016/j.envint.2019.02.048
169. Li H, Huang K, Jin S, et al. Environmental cadmium exposure induces alterations in the urinary metabolic profile of pregnant women. *Int J Hyg Environ Health*. Apr 2019;222(3):556-562. doi:10.1016/j.ijheh.2019.02.007
170. Chu H, Huang FQ, Yuan Q, et al. Metabolomics identifying biomarkers of PM2.5 exposure for vulnerable population: based on a prospective cohort study. *Environ Sci Pollut Res Int*. Mar 2021;28(12):14586-14596. doi:10.1007/s11356-020-11677-0
171. Walker C, Garza S, Papadopoulos V, Culty M. Impact of endocrine-disrupting chemicals on steroidogenesis and consequences on testicular function. *Mol Cell Endocrinol*. May 1 2021;527:111215. doi:10.1016/j.mce.2021.111215
172. Baker MG, Simpson CD, Lin YS, Shireman LM, Seixas N. The Use of Metabolomics to Identify Biological Signatures of Manganese Exposure. *Ann Work Expo Health*. May 1 2017;61(4):406-415. doi:10.1093/annweh/wxw032
173. Wang M, Rang O, Liu F, et al. A systematic review of metabolomics biomarkers for Bisphenol A exposure. *Metabolomics*. Mar 5 2018;14(4):45. doi:10.1007/s11306-018-1342-z
174. Guo P, Furnary T, Vasiliou V, et al. Non-targeted metabolomics and associations with per- and polyfluoroalkyl substances (PFAS) exposure in humans: A scoping review. *Environ Int*. Apr 2022;162:107159. doi:10.1016/j.envint.2022.107159
175. Li S, Cirillo P, Hu X, et al. Understanding mixed environmental exposures using metabolomics via a hierarchical community network model in a cohort of California women in 1960's. *Reprod Toxicol*. Mar 2020;92:57-65. doi:10.1016/j.reprotox.2019.06.013
176. Bingol K, Bruschweiler R. Knowns and unknowns in metabolomics identified by multidimensional NMR and hybrid MS/NMR methods. *Curr Opin Biotechnol*. Feb 2017;43:17-24. doi:10.1016/j.copbio.2016.07.006

177. Wishart DS. Advances in metabolite identification. *Bioanalysis*. Aug 2011;3(15):1769-82. doi:10.4155/bio.11.155
178. Boccard J, Veuthey JL, Rudaz S. Knowledge discovery in metabolomics: an overview of MS data handling. *J Sep Sci*. Feb 2010;33(3):290-304. doi:10.1002/jssc.200900609
179. Caesar LK, Kellogg JJ, Kvalheim OM, Cech NB. Opportunities and Limitations for Untargeted Mass Spectrometry Metabolomics to Identify Biologically Active Constituents in Complex Natural Product Mixtures. *J Nat Prod*. Mar 22 2019;82(3):469-484. doi:10.1021/acs.jnatprod.9b00176
180. Bevilacqua M, Bro R. Can We Trust Score Plots? *Metabolites*. Jul 8 2020;10(7)doi:10.3390/metabo10070278
181. Richman T, Arnold E, Williams AJ. Curation of a list of chemicals in biosolids from EPA National Sewage Sludge Surveys & Biennial Review Reports. *Sci Data*. Apr 19 2022;9(1):180. doi:10.1038/s41597-022-01267-9
182. Rhind SM, Kyle CE, Owen J. Accumulation of potentially toxic metals in the liver tissue of sheep grazed on sewage sludge-treated pastures. *Animal Science*. 2005;81(1):107-113. doi:10.1079/ASC42120107
183. Fries GF. A review of the significance of animal food products as potential pathways of human exposures to dioxins. *J Anim Sci*. Jun 1995;73(6):1639-50. doi:10.2527/1995.7361639x
184. Blumenthal JM, Baltensperger DD, Cassman KG, Mason SC, Pavlista AD. Chapter 3 - Importance and Effect of Nitrogen on Crop Quality and Health. In: Hatfield JL, Follett RF, eds. *Nitrogen in the Environment (Second Edition)*. Academic Press; 2008:51-70.
185. Ladd-Acosta C. Epigenetic Signatures as Biomarkers of Exposure. *Curr Environ Health Rep*. Jun 2015;2(2):117-25. doi:10.1007/s40572-015-0051-2
176. Graphical abstract was created using biorender.com using the creative commons images - "Delivering biosolids, Goulburn NSW" by NSW DPI Schools program is licensed under CC BY-NC-SA 2.0 and "Greener pastures" by Vince Alongi is licensed under CC BY 2.0.

Figure Captions:

Figure 1: Multi-variate analyses of known metabolites in maternal plasma of all animals in control (n=15) and BTP (n=13) groups. The top panel represents principal component analysis score plots from negative ion mode (left) and positive ion mode (right) and the bottom panel shows orthogonal projections to latent structures discriminant analysis score plot from negative ion mode (left) and positive ion mode (right) showing separation based on serum metabolites. Each point represents one animal, and the ellipse indicates 95% confidence intervals.

Figure 2: Differential Metabolites. (a) Pie-chart of distribution of the differential metabolite classes. (b) Pie-chart of different sub-classes of lipids and lipid-like molecules (c) Pie-chart of different sub classes of organic acids and derivatives. (d) Pathway analysis based on the differential metabolites. X-axis shows the -log P values from the pathway enrichment analysis. The node color and radius are based on its P value and enrichment ratio, respectively.

Figure 3: Effect of Biosolids exposure on different classes of differential metabolites. The bar graph represents peak intensities of different sub classes of metabolites between the control (n=15) and BTP (n=13) groups. ** $P < 0.001$ Mann-Whitney U test with Benjamini Hochberg correction. Figures represent summary of all differential metabolites grouped together; levels of individual metabolites of functional significance are represented in figures 4 and 5.

Figure 4: Effect of Biosolids exposure on different sub-classes of lipids. Bar graph represents peak intensities of differential metabolites of the lipid super-class between control (n=15) and BTP (n=13) groups *$P < 0.05$ ** $P < 0.001$ Mann-Whitney U test with Benjamini Hochberg correction.

Figure 5: Effect of Biosolids exposure on different sub-classes of amino acids. Bar graph represents peak intensities of differential metabolites belonging to different amino acid pathways between the control (n=15) and BTP (n=13) groups *P < 0.05 ** P < 0.001 Mann-Whitney U test with Benjamini Hochberg correction.

Figure 6: Potential markers of biosolids exposure in plasma. (a) OPLS-DA S-plot of metabolites from maternal plasma showing potential metabolite markers of biosolid exposure. The up and down arrows indicate metabolites with elevated and decreased levels in response to biosolid exposure, respectively. Each point represents a metabolite. (b) Top 25 differential metabolites identified by OPLS-DA according to the VIP score on the x-axis. The relative concentration of the metabolite in each group is indicated by the colored boxes on the right with blue and red indicating lower and higher concentrations, respectively. C-Control, BTP- biosolid treated pasture. (c) Heat maps of the top 25 significant differential metabolites based on the t-test. Individual animals from Control and BTP groups are represented on the x-axis and the metabolites on the y-axis. Red represents higher and blue represents lower concentrations of the metabolite.

Figure 7: Fetal sex-specific analysis of metabolites. Multi-variate analyses of known metabolites in maternal plasma of (a) animals with male fetus only and (b) animals with female fetus only. In both (a) and (b), the top panel represents principal component analysis score plots from negative ion mode (left) and positive ion mode (right) and the bottom panel shows orthogonal projections to latent structures discriminant analysis score plot from negative ion mode (left) and positive ion mode (right) showing separation based on serum metabolites. Each point represents one animal, and the ellipse indicates 95%

confidence intervals. (c) Effect of Biosolids exposure on different classes of differential metabolites based on fetal sex. The bar graph represents peak intensities of different sub classes of metabolites between the control and BTP groups in animals with male fetus (control, n = 9; BTP, n = 5) and animals with female fetus or female fetus only (control, n = 5; BTP, n = 7). *P < 0.05 **P < 0.01, *** P < 0.001 by two-way ANOVA with Tukey's multiple comparison test.

Supplementary Figure Captions:

Figure S1: (a) Principal Component Analysis score plots from negative ion mode (left) and positive ion mode (right) based on plasma metabolites from a. all animals in control and BTP groups, including two outliers from the BTP group that lie outside the 95% confidence interval margin. (b) Multivariate analysis using SIMCA. The top panel represents principal component analysis score plots from negative ion mode (left) and positive ion mode (right) and the bottom panel shows orthogonal projections to latent structures discriminant analysis score plot from negative ion mode (left) (R^2Y= 0.97, Q^2 = 0.81) and positive ion mode (right) (R^2Y= 0.99, Q^2 = 0.93) showing separation based on serum metabolites. Each point represents one animal, and the ellipse indicates 95% confidence intervals.

Figure S2. (a) Heat maps of the top 25 significant differential metabolites in negative (left) and positive (right) mode. Individual animals from control (n=15) and BTP (n=13) groups are represented on the x-axis and metabolites on the Y-axis. Red represents higher and blue represents lower expression of the metabolite. (b) The top 25 differential metabolites identified by OPLS-DA in the negative (left) and positive (right) ion modes, according to the VIP score on the x-axis. The relative concentration of the

metabolite in each group is indicated by the colored boxes on the right with blue and red indicating lower and higher concentrations, respectively.

Figure S3: Heatmap of differential metabolites belonging to the sub class of lipids and lipid like molecules grouped according to their sub-class. Individual animals are represented on the x-axis and metabolites on the y-axis. Red represents higher and blue represents lower concentrations of the metabolite in BTP samples compared to control samples. The different sub-class of lipids are indicated on the left.

Figure S4: Heatmap of differential metabolites belonging to the sub class of organic acids and derivatives. Individual animals are represented on the x-axis and the metabolites on the y-axis. Red represents higher and blue represents lower concentration of the metabolite.

Figure S5: Heatmap of differential metabolites belonging to the sub class of (a) nucleotides and analogues, (b) alkaloids, (c) phenylpropanoids and polyketides, and (d) organic compounds including organo-heterocyclic, organic nitrogen, organic oxygen and organo-sulfur compounds. Individual animals are represented on the x-axis and the metabolites on the y-axis. Red represents higher and blue represents lower concentration of the metabolite.

Figure S6: Top figure shows heatmap of differential metabolites belonging to the sub class of Benzenoids. Individual animals are represented on the x-axis and metabolites on the y-axis. Red represents higher and blue represents lower expression of the metabolite. Bottom figure represents the Correlation Network between the differential metabolites. Each node indicates a differential metabolite and thickness of lines

represent the strength of the correlation. The differential metabolites of the benzenoid class are indicated by *.

Figure S7: Fetal sex-specific analysis of metabolites using SIMCA. (a) Multi-variate analyses of known metabolites in maternal plasma of animals with male fetuses only. The top panel represents principal component analysis score plots from negative ion mode (left) and positive ion mode (right) and the bottom panel shows orthogonal projections to latent structures discriminant analysis score plot from negative ion mode (left) ($R^2Y= 1$, $Q^2 = 0.72$) and positive ion mode (right) (($R^2Y= 1$, $Q^2 = 0.75$) showing separation based on serum metabolites (b) Multi-variate analyses of known metabolites in maternal plasma of animals with female fetuses only. The top panel represents principal component analysis score plots from negative ion mode (left) and positive ion mode (right) and the bottom panel shows orthogonal projections to latent structures discriminant analysis score plot from negative ion mode (left) ($R^2Y= 0.99$, $Q^2 = 0.69$) and positive ion mode (right) ($R^2Y= 1$, $Q^2 = 0.84$) showing separation based on serum metabolites. Each point represents one animal, and the ellipse indicates 95% confidence intervals.

Figure S8: Differential metabolites identified in ewes carrying male fetuses (control, n= 9 and BTP, n= 5). Red represents higher and blue represents lower concentrations of the metabolite.

Figure S9: Differential metabolites in ewes carrying female fetuses. (Control, n= 5 and BTP, n= 7) VIP score plot and heat-map of metabolites. (a) Top 25 differential metabolites identified by OPLS-DA in ewes carrying a female fetus according to the VIP score on the x-axis. The relative concentration of the metabolite in each group is indicated by the colored boxes on the right. (b) Heat map of the top 25 significant differential metabolites in ewes carrying a female fetus. The samples are represented on the x-

axis and metabolites on the y-axis. Red represents a higher concentration and blue represents lower concentration of the metabolite.

Table Legends:

Table 1: Top 10 differentially abundant metabolites identified from the negative ion mode and positive ion mode

Supplementary Table S1: Differentially abundant metabolites between Control and BTP groups of all animals

Supplementary Table S2: Descriptive statistics for Control and BTP comparison

Supplementary Table S3: Differentially abundant exogenous metabolites and their source

Supplementary Table S4: Differentially abundant metabolites between Control and BTP groups of ewes carrying male fetuses

Supplementary Table S5: Differentially abundant metabolites between Control and BTP groups of ewes carrying female fetuses

Supplementary Table S6: Descriptive statistics for Control and BTP comparison based on fetal sex

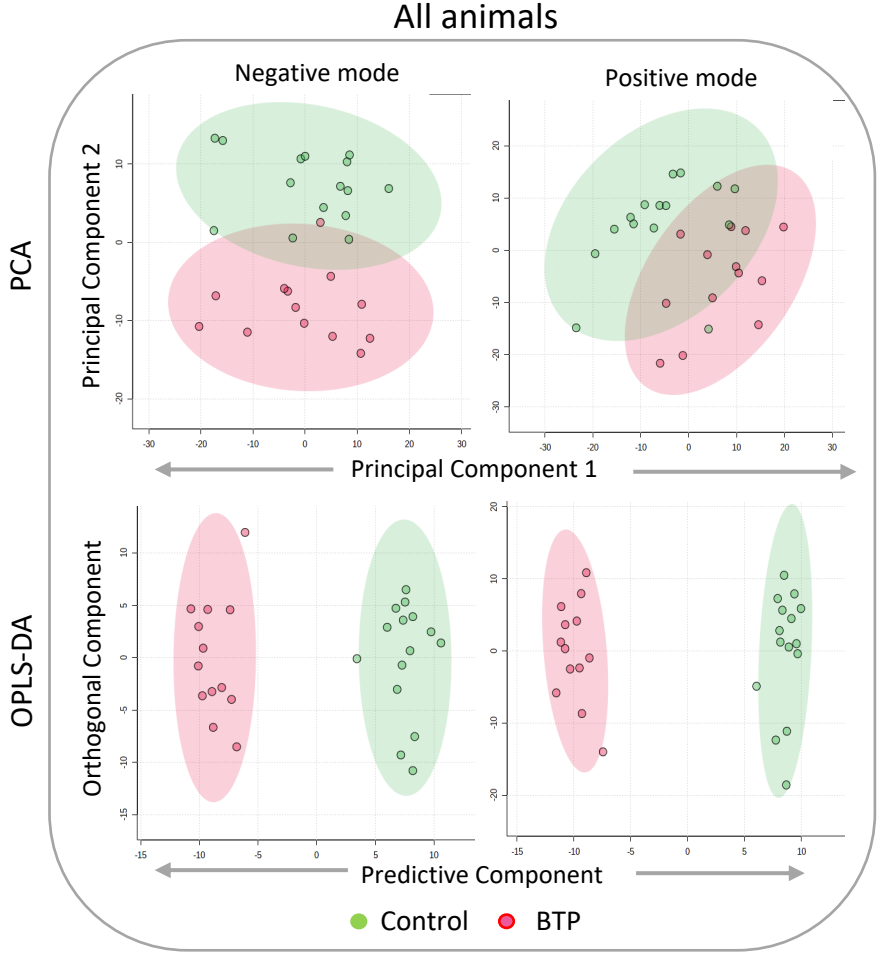
All animals
Negative mode
Positive mode
PCA
Principal Component 2
Principal Component 1
OPLS-DA
Orthogonal Component
Predictive Component
Control
BTP

a. Classification of Differential Metabolites

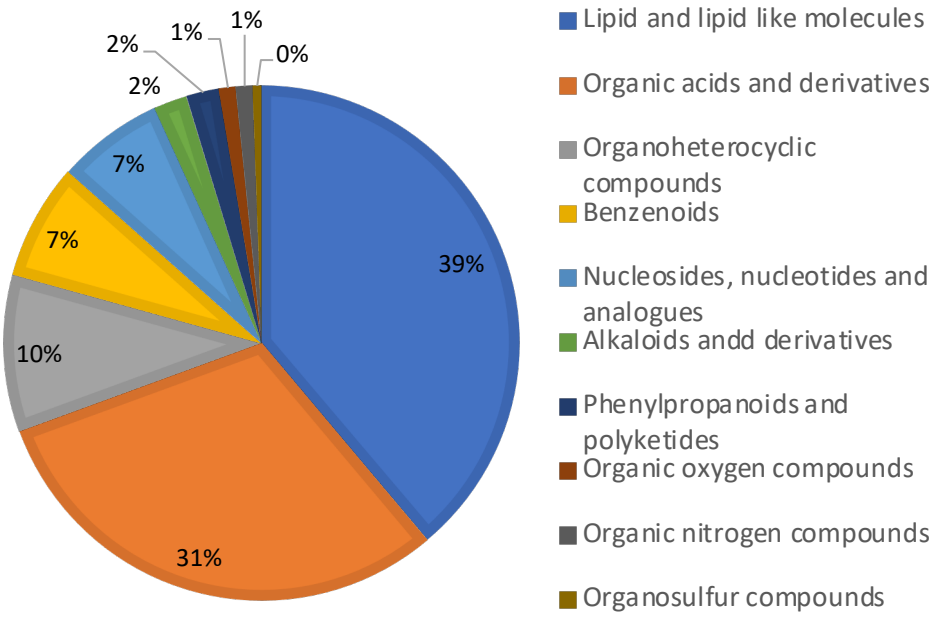

b. Lipids and lipid-like molecules

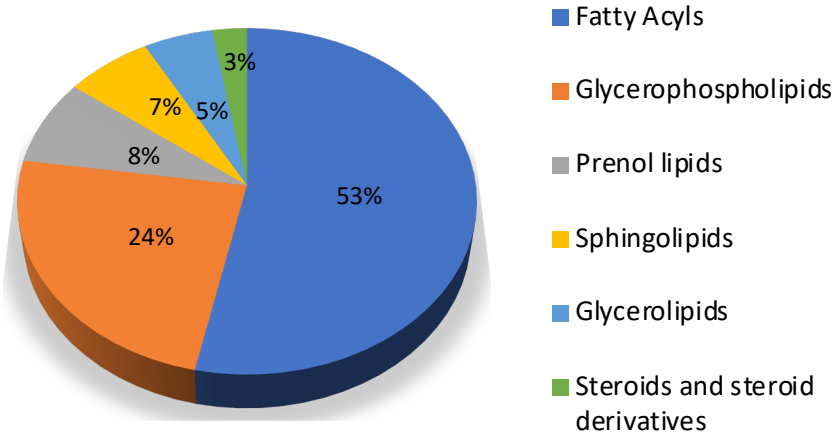

c. Organic acids and derivatives

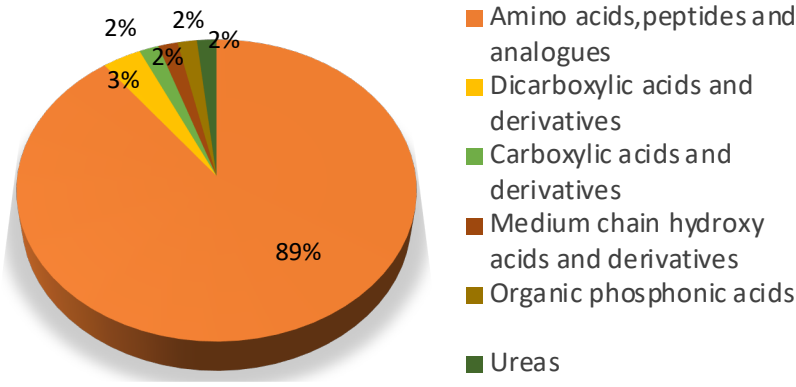

d. Pathway analysis based on differential metabolites

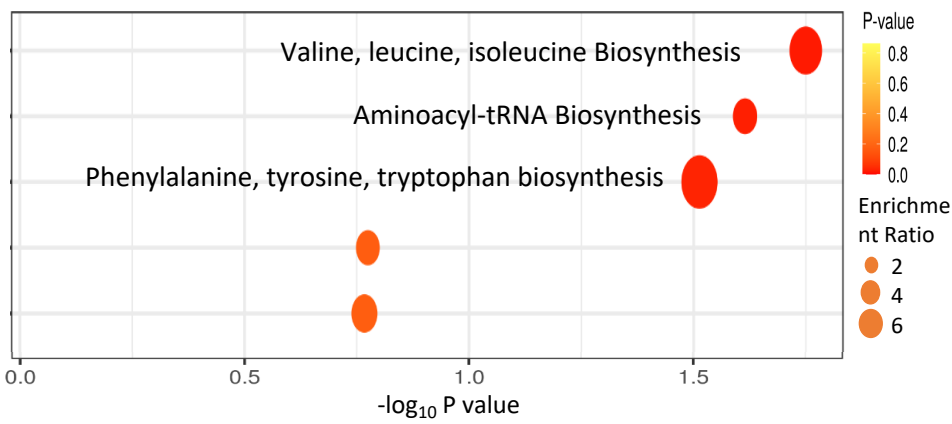

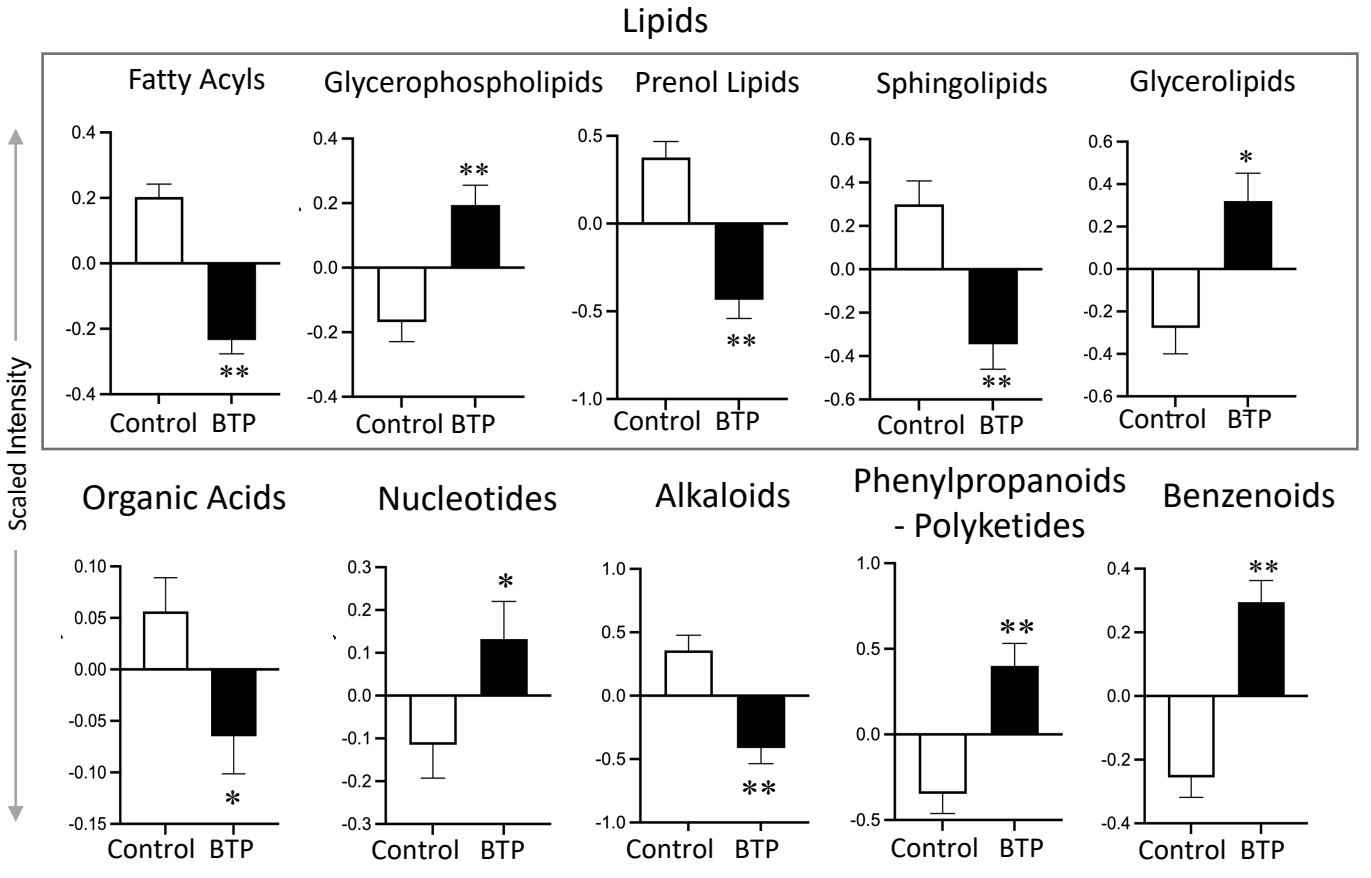
Lipids
Fatty Acyls
Glycerophospholipids
Prenol Lipids
Sphingolipids
Glycerolipids
Scaled Intensity
Control BTP
Organic Acids
Nucleotides
Alkaloids
Phenylpropanoids - Polyketides
Benzenoids

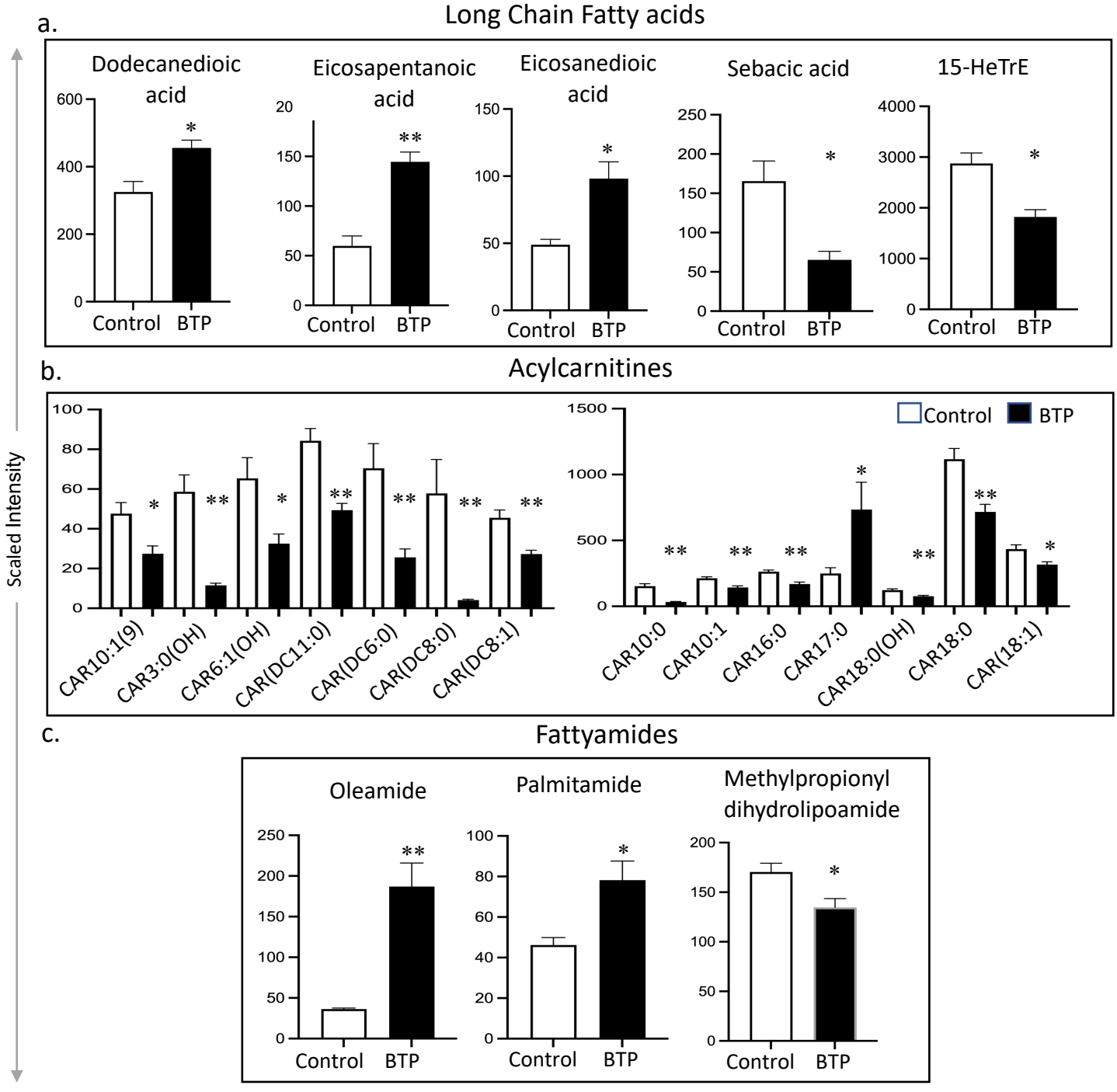
a.
Long Chain Fatty acids
Dodecanedioic acid
Eicosapentanoic acid
Eicosanedioic acid
Sebacic acid
15-HeTrE
Control
BTP
b.
Acylcarnitines
Control
BTP
CAR10:1(9)
CAR3:0(OH)
CAR6:1(OH)
CAR(DC11:0)
CAR(DC6:0)
CAR(DC8:0)
CAR(DC8:1)
CAR10:0
CAR10:1
CAR16:0
CAR17:0
CAR18:0(OH)
CAR18:0
CAR(18:1)
Scaled Intensity
c.
Fattyamides
Oleamide
Palmitamide
Methylpropionyl dihydrolipoamide

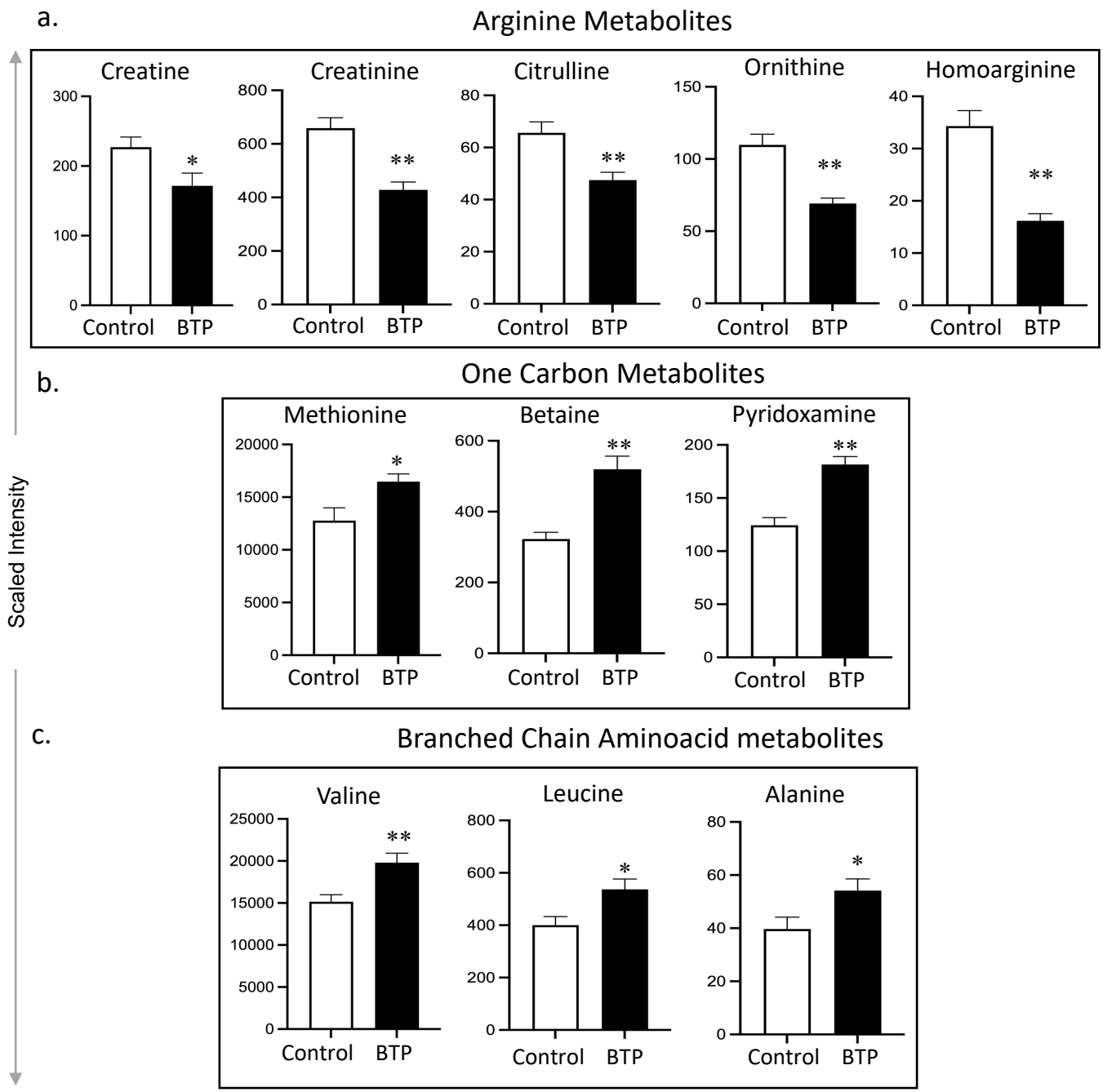
a.
Arginine Metabolites
Creatine
Creatinine
Citrulline
Ornithine
Homoarginine
Control
BTP
b.
One Carbon Metabolites
Methionine
Betaine
Pyridoxamine
Scaled Intensity
c.
Branched Chain Aminoacid metabolites
Valine
Leucine
Alanine

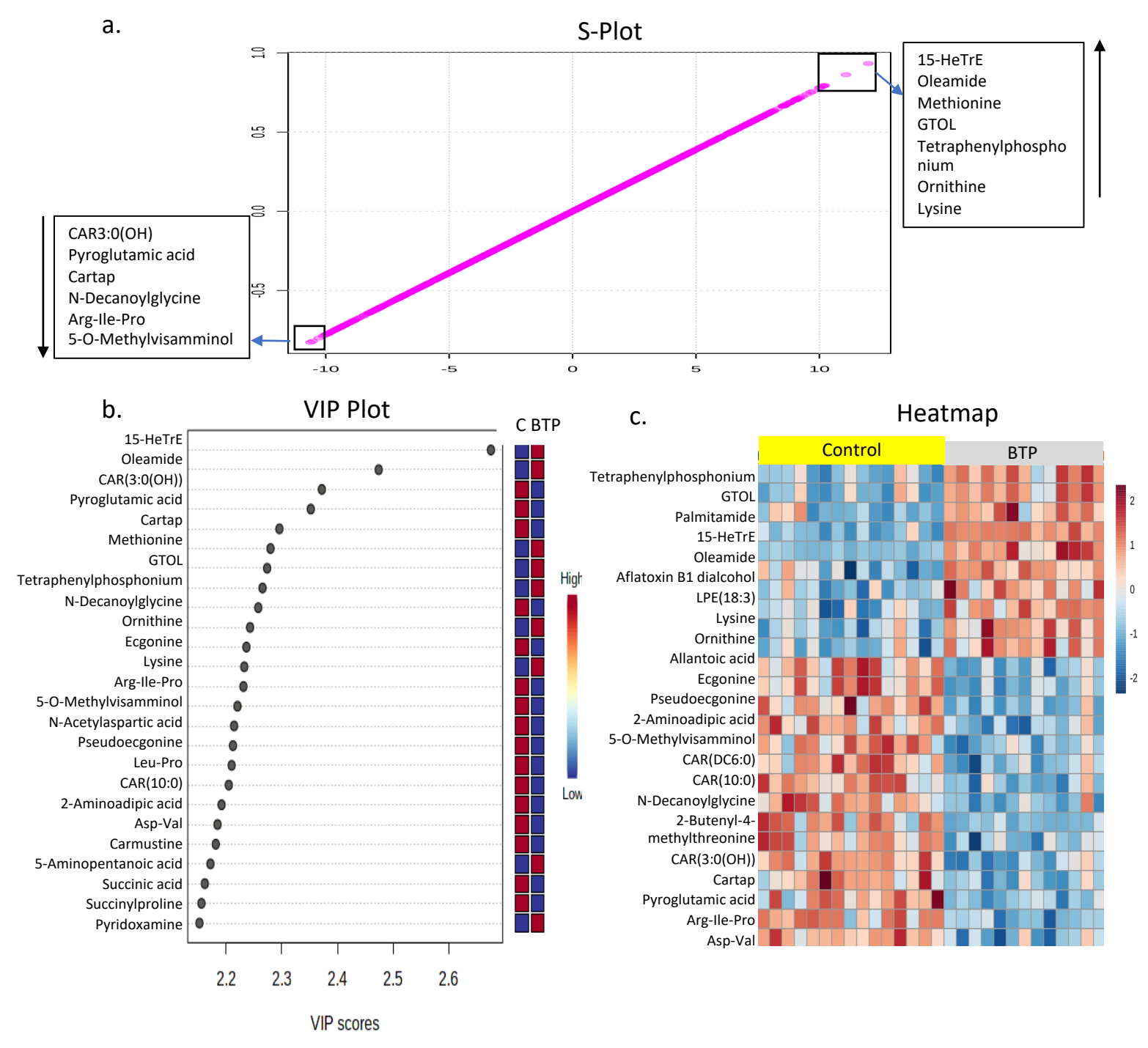
a.
S-Plot
15-HeTrE
Oleamide
Methionine
GTOL
Tetraphenylphospho nium
Ornithine
Lysine
CAR3:0(OH)
Pyroglutamic acid
Cartap
N-Decanoylglycine
Arg-Ile-Pro
5-O-Methylvisamminol
1.0
0.5
0.0
-0.5
-10
-5
0
5
10
b.
VIP Plot
C BTP
15-HeTrE
Oleamide
CAR(3:0(OH))
Pyroglutamic acid
Cartap
Methionine
GTOL
Tetraphenylphosphonium
N-Decanoylglycine
Ornithine
Ecgonine
Lysine
Arg-Ile-Pro
5-O-Methylvisamminol
N-Acetylaspartic acid
Pseudoecgonine
Leu-Pro
CAR(10:0)
2-Aminoadipic acid
Asp-Val
Carmustine
5-Aminopentanoic acid
Succinic acid
Succinylproline
Pyridoxamine
High
Low
2.2
2.3
2.4
2.5
2.6
VIP scores
c.
Heatmap
Control
BTP
Tetraphenylphosphonium
GTOL
Palmitamide
15-HeTrE
Oleamide
Aflatoxin B1 dialcohol
LPE(18:3)
Lysine
Ornithine
Allantoic acid
Ecgonine
Pseudoecgonine
2-Aminoadipic acid
5-O-Methylvisamminol
CAR(DC6:0)
CAR(10:0)
N-Decanoylglycine
2-Butenyl-4-methylthreonine
CAR(3:0(OH))
Cartap
Pyroglutamic acid
Arg-Ile-Pro
Asp-Val
2
1
0
-1
-2

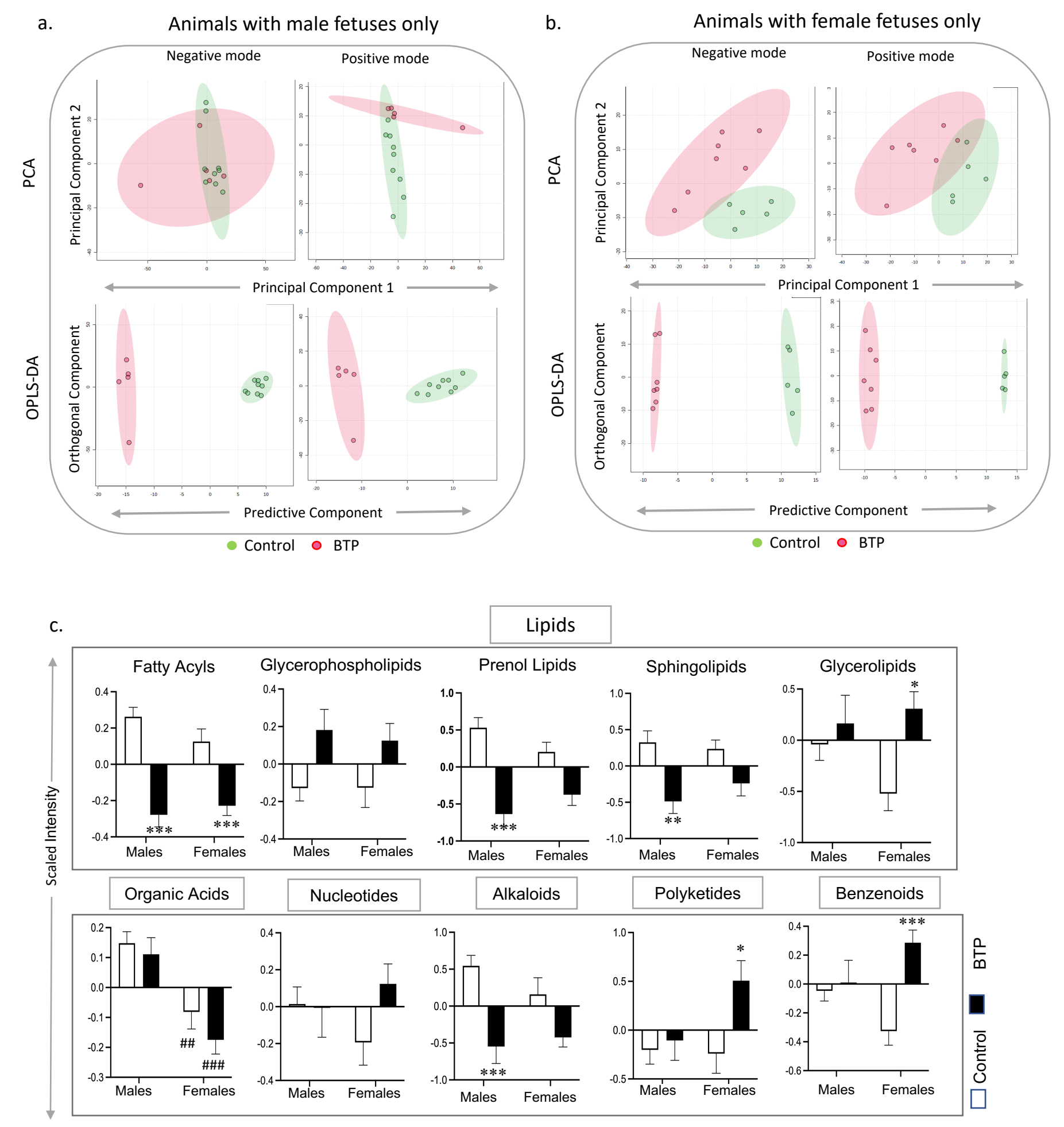
a.
Animals with male fetuses only
Negative mode
Positive mode
PCA
Principal Component 2
Principal Component 1
OPLS-DA
Orthogonal Component
Predictive Component
Control
BTP
b.
Animals with female fetuses only
Negative mode
Positive mode
PCA
Principal Component 2
Principal Component 1
OPLS-DA
Orthogonal Component
Predictive Component
Control
BTP
c.
Lipids
Fatty Acyls
Glycerophospholipids
Prenol Lipids
Sphingolipids
Glycerolipids
Scaled Intensity
Organic Acids
Nucleotides
Alkaloids
Polyketides
Benzenoids
Males
Females
BTP
Control

Summary Figure

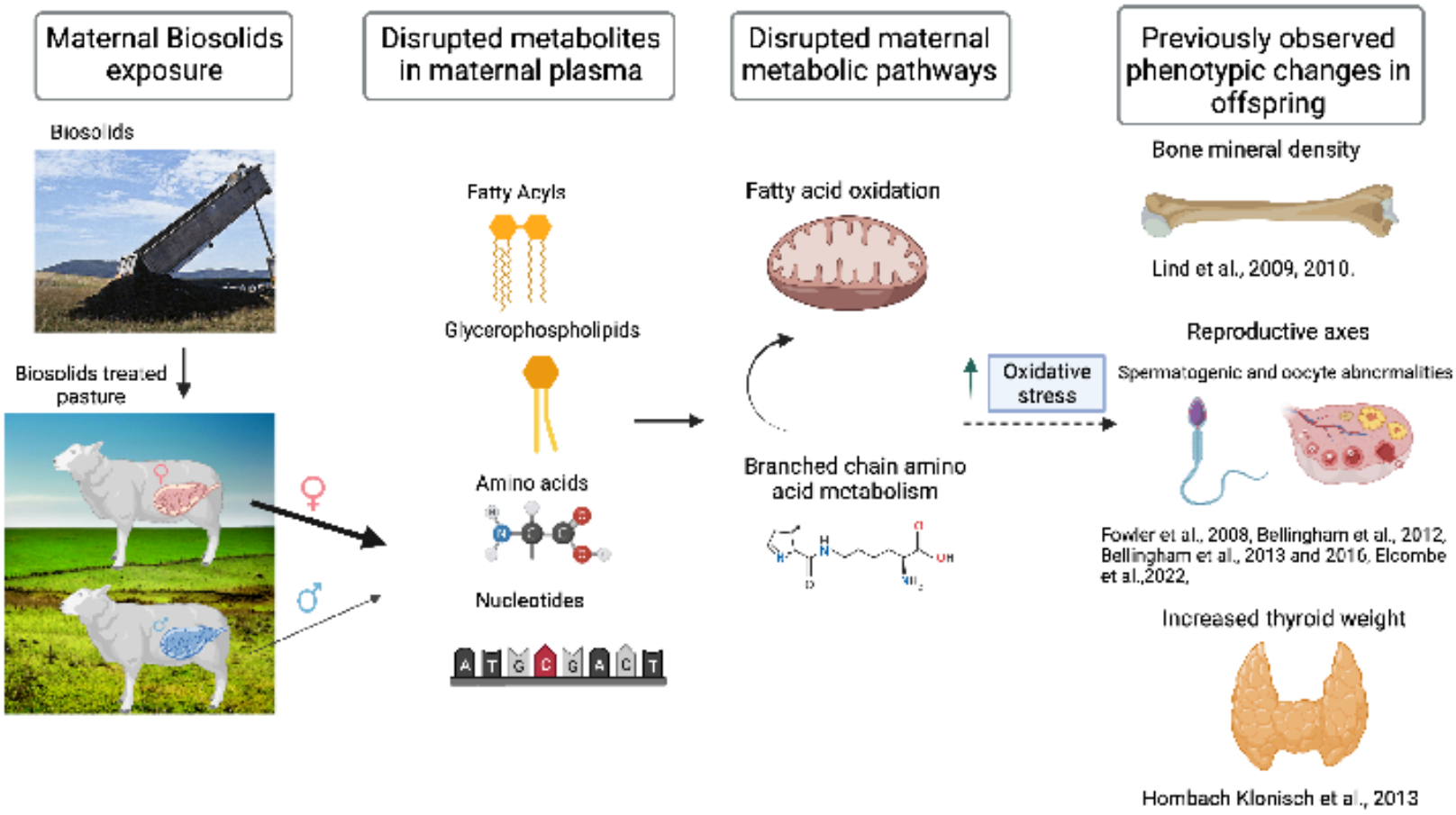

a.

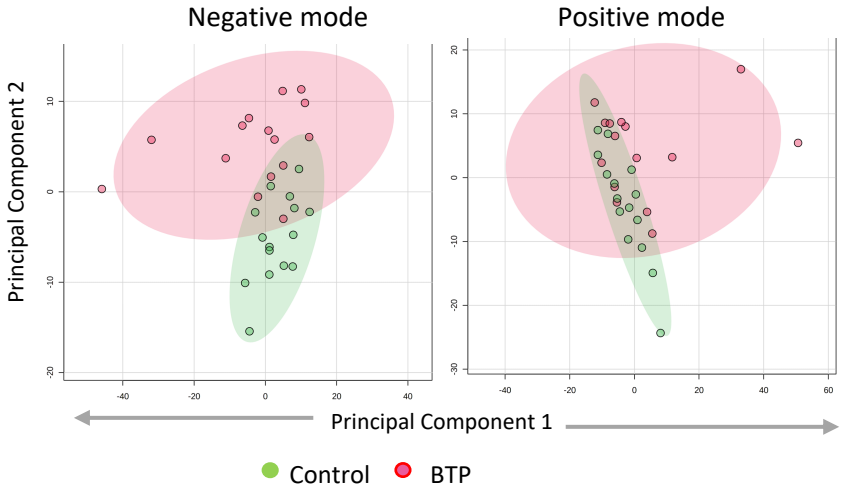
Negative mode
Positive mode
Principal Component 2
Principal Component 1
Control
BTP

b.

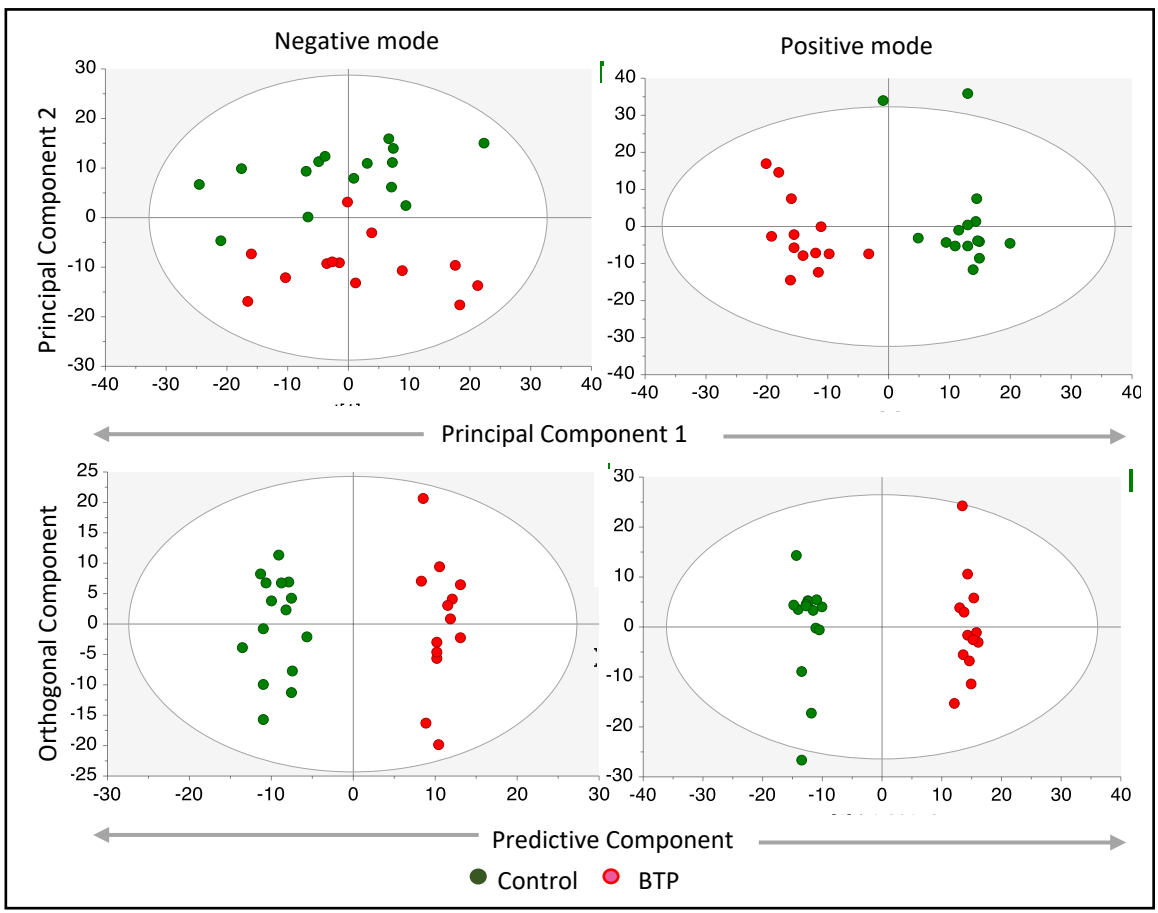
All animals
Negative mode
Positive mode
PCA
OPLS-DA
Principal Component 2
Principal Component 1
Orthogonal Component
Predictive Component
Control
BTP

a.

Heatmap

Negative mode

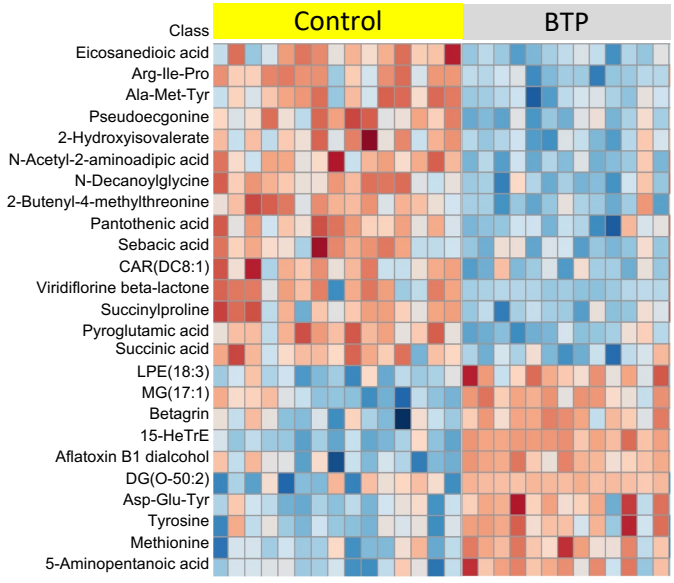

Positive mode

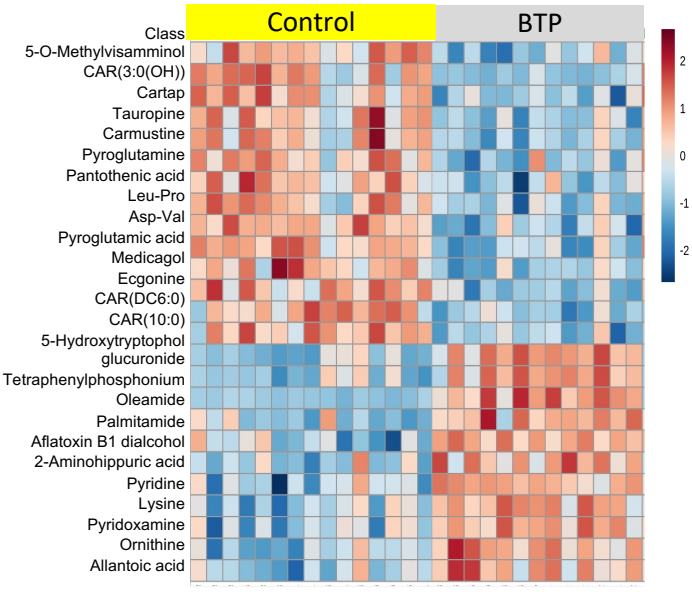

b.

VIP Plot

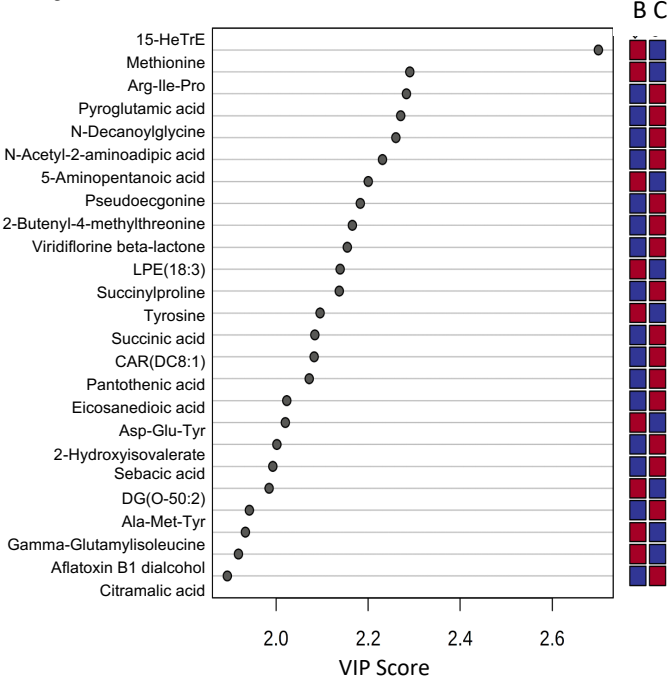

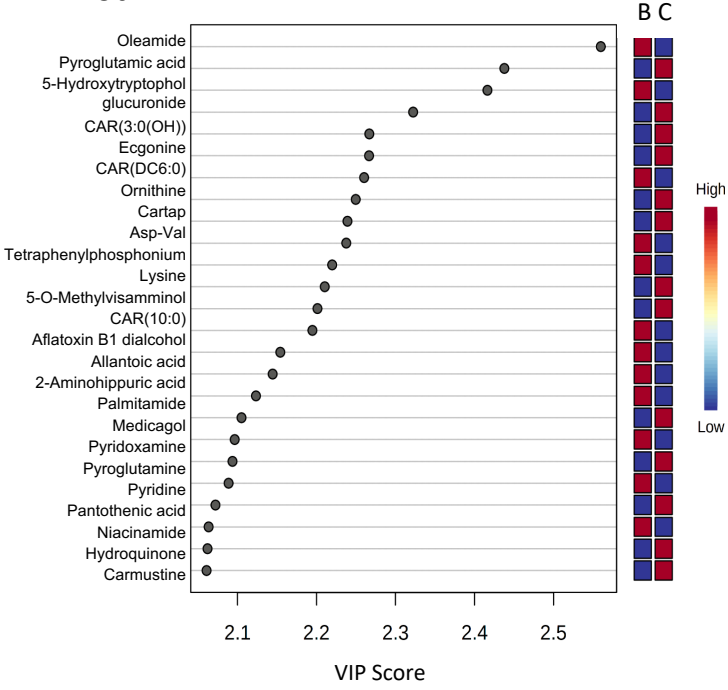

Figure S3.

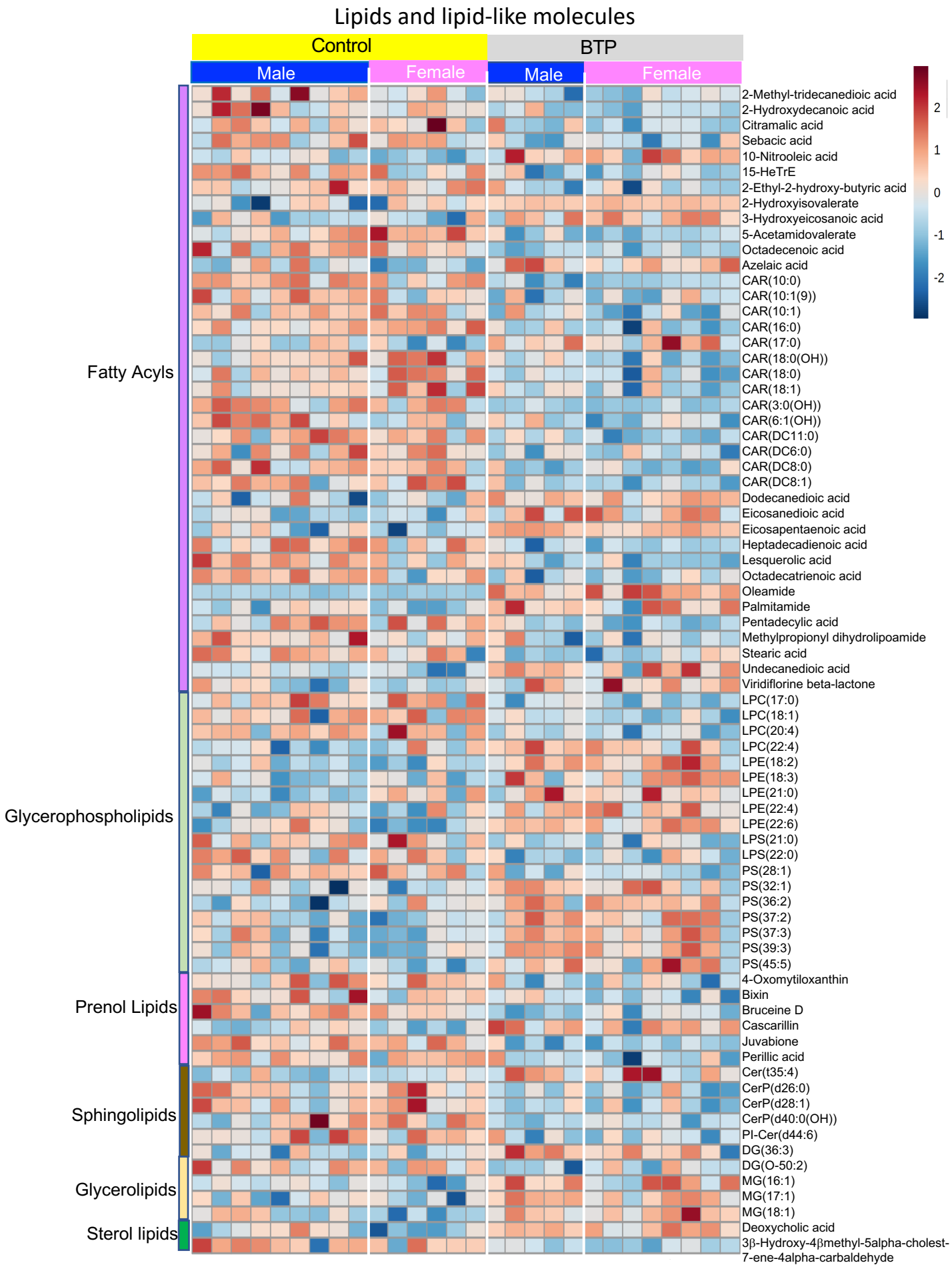
Lipids and lipid-like molecules
Control
BTP
Male
Female
Male
Female
Fatty Acyls
Glycerophospholipids
Prenol Lipids
Sphingolipids
Glycerolipids
Sterol lipids
2-Methyl-tridecanedioic acid
2-Hydroxydecanoic acid
Citramalic acid
Sebacic acid
10-Nitrooleic acid
15-HeTrE
2-Ethyl-2-hydroxy-butyric acid
2-Hydroxyisovalerate
3-Hydroxyeicosanoic acid
5-Acetamidovalerate
Octadecenoic acid
Azelaic acid
CAR(10:0)
CAR(10:1(9))
CAR(10:1)
CAR(16:0)
CAR(17:0)
CAR(18:0(OH))
CAR(18:0)
CAR(18:1)
CAR(3:0(OH))
CAR(6:1(OH))
CAR(DC11:0)
CAR(DC6:0)
CAR(DC8:0)
CAR(DC8:1)
Dodecanedioic acid
Eicosanedioic acid
Eicosapentaenoic acid
Heptadecadienoic acid
Lesquerolic acid
Octadecatrienoic acid
Oleamide
Palmitamide
Pentadecylic acid
Methylpropionyl dihydrolipoamide
Stearic acid
Undecanedioic acid
Viridiflorine beta-lactone
LPC(17:0)
LPC(18:1)
LPC(20:4)
LPC(22:4)
LPE(18:2)
LPE(18:3)
LPE(21:0)
LPE(22:4)
LPE(22:6)
LPS(21:0)
LPS(22:0)
PS(28:1)
PS(32:1)
PS(36:2)
PS(37:2)
PS(37:3)
PS(39:3)
PS(45:5)
4-Oxomytiloxanthin
Bixin
Bruceine D
Cascarillin
Juvabione
Perillic acid
Cer(t35:4)
CerP(d26:0)
CerP(d28:1)
CerP(d40:0(OH))
PI-Cer(d44:6)
DG(36:3)
DG(O-50:2)
MG(16:1)
MG(17:1)
MG(18:1)
Deoxycholic acid
3β-Hydroxy-4βmethyl-5alpha-cholest-7-ene-4alpha-carbaldehyde
2
1
0
-1
-2

Figure S4

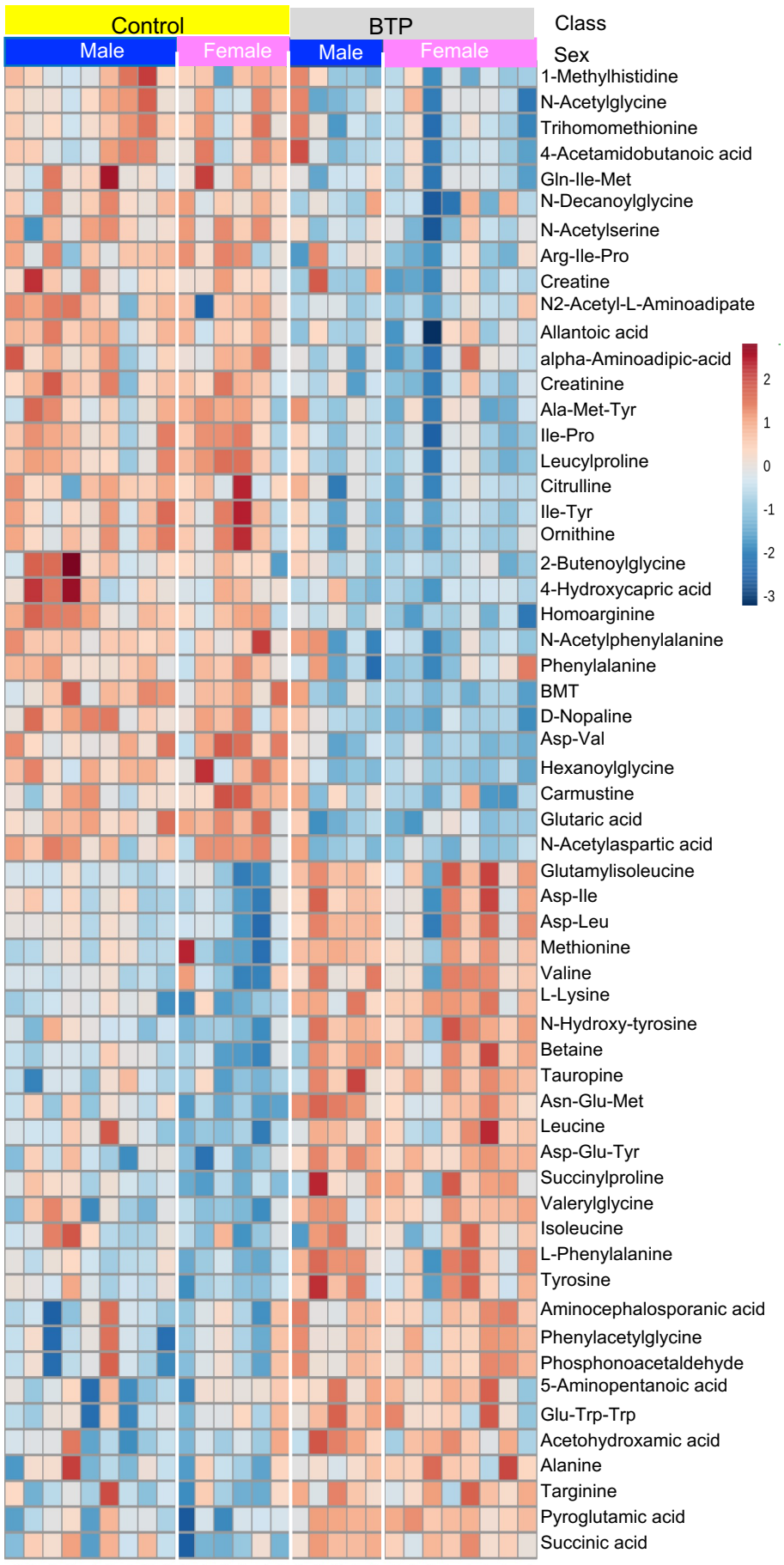
Organic acids and derivatives
Control
BTP
Class
Male
Female
Male
Female
Sex
1-Methylhistidine
N-Acetylglycine
Trihomomethionine
4-Acetamidobutanoic acid
Gln-Ile-Met
N-Decanoylglycine
N-Acetylserine
Arg-Ile-Pro
Creatine
N2-Acetyl-L-Aminoadipate
Allantoic acid
alpha-Aminoadipic-acid
Creatinine
Ala-Met-Tyr
Ile-Pro
Leucylproline
Citrulline
Ile-Tyr
Ornithine
2-Butenoylglycine
4-Hydroxycapric acid
Homoarginine
N-Acetylphenylalanine
Phenylalanine
BMT
D-Nopaline
Asp-Val
Hexanoylglycine
Carmustine
Glutaric acid
N-Acetylaspartic acid
Glutamylisoleucine
Asp-Ile
Asp-Leu
Methionine
Valine
L-Lysine
N-Hydroxy-tyrosine
Betaine
Tauropine
Asn-Glu-Met
Leucine
Asp-Glu-Tyr
Succinylproline
Valerylglycine
Isoleucine
L-Phenylalanine
Tyrosine
Aminocephalosporanic acid
Phenylacetylglycine
Phosphonoacetaldehyde
5-Aminopentanoic acid
Glu-Trp-Trp
Acetohydroxamic acid
Alanine
Targinine
Pyroglutamic acid
Succinic acid
2
1
0
-1
-2
-3

Figure S5

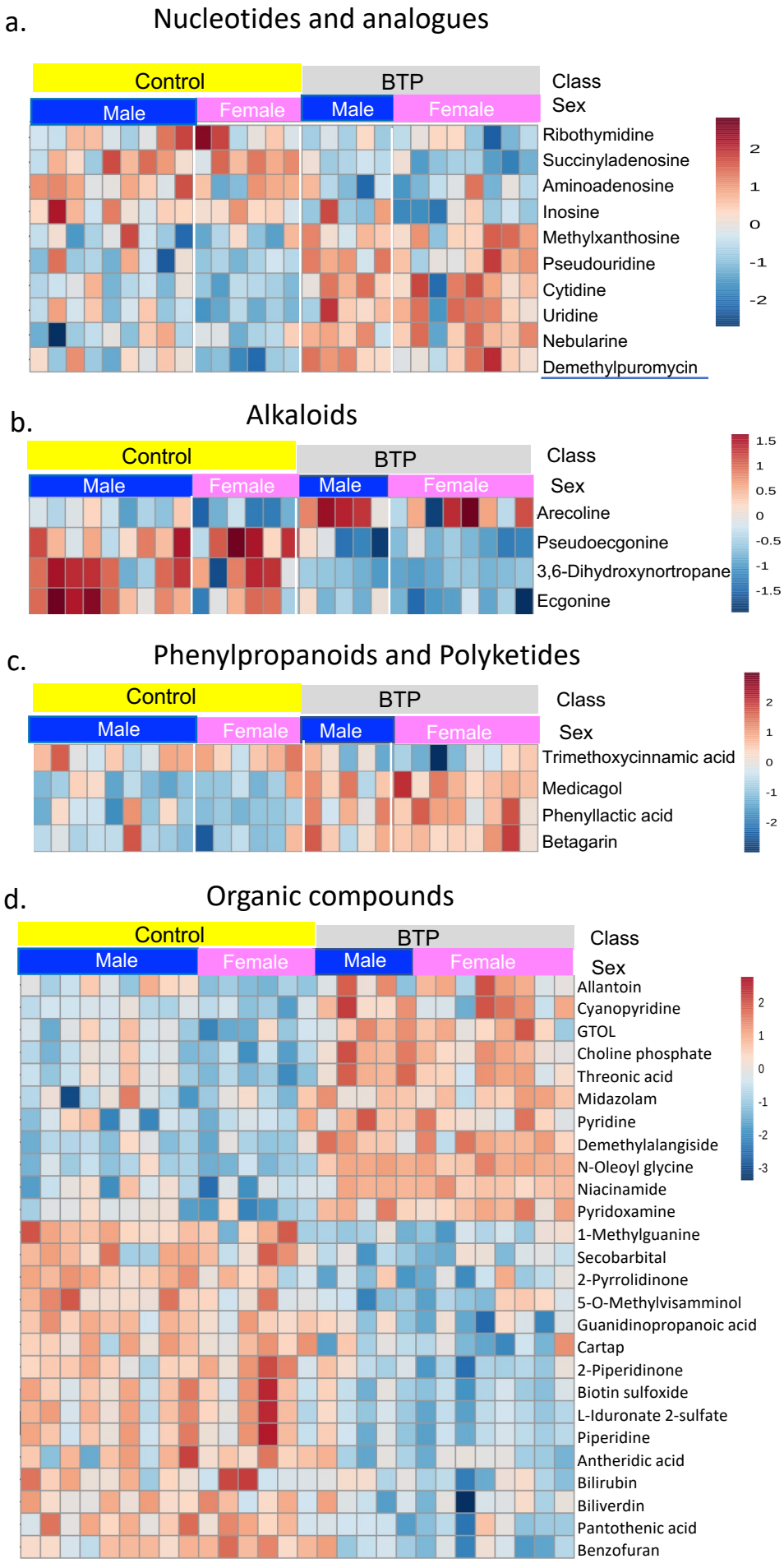
a.
Nucleotides and analogues
Control
BTP
Class
Male
Female
Male
Female
Sex
Ribothymidine
Succinyladenosine
Aminoadenosine
Inosine
Methylxanthosine
Pseudouridine
Cytidine
Uridine
Nebularine
Demethylpuromycin
2
1
0
-1
-2
b.
Alkaloids
Control
BTP
Class
Male
Female
Male
Female
Sex
Arecoline
Pseudoecgonine
3,6-Dihydroxynortropane
Ecgonine
1.5
1
0.5
0
-0.5
-1
-1.5
c.
Phenylpropanoids and Polyketides
Control
BTP
Class
Male
Female
Male
Female
Sex
Trimethoxycinnamic acid
Medicagol
Phenyllactic acid
Betagarin
2
1
0
-1
-2
d.
Organic compounds
Control
BTP
Class
Male
Female
Male
Female
Sex
Allantoin
Cyanopyridine
GTOL
Choline phosphate
Threonic acid
Midazolam
Pyridine
Demethylalangiside
N-Oleoyl glycine
Niacinamide
Pyridoxamine
1-Methylguanine
Secobarbital
2-Pyrrolidinone
5-O-Methylvisamminol
Guanidinopropanoic acid
Cartap
2-Piperidinone
Biotin sulfoxide
L-Iduronate 2-sulfate
Piperidine
Antheridic acid
Bilirubin
Biliverdin
Pantothenic acid
Benzofuran
2
1
0
-1
-2
-3

Figure S6

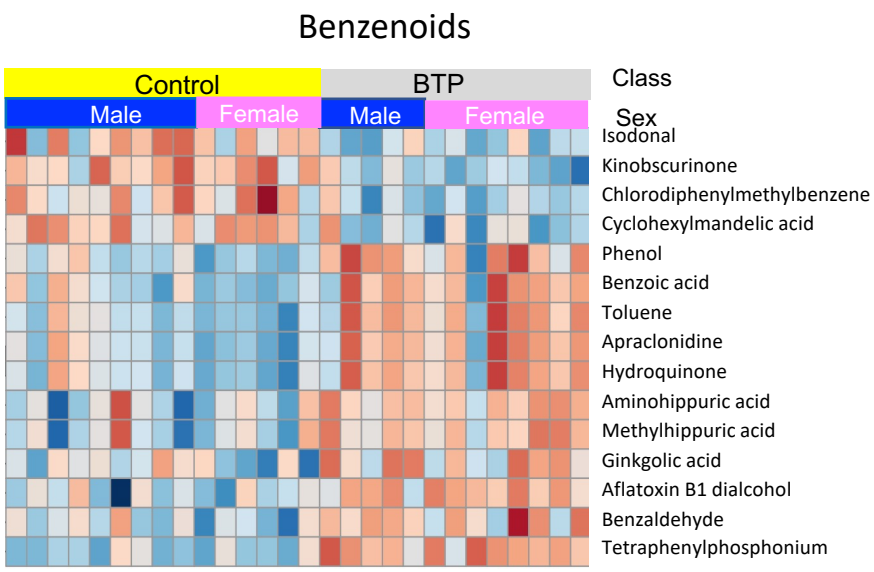
Benzenoids
Control
BTP
Class
Male
Female
Male
Female
Sex
Isodonal
Kinobscurinone
Chlorodiphenylmethylbenzene
Cyclohexylmandelic acid
Phenol
Benzoic acid
Toluene
Apraclonidine
Hydroquinone
Aminohippuric acid
Methylhippuric acid
Ginkgolic acid
Aflatoxin B1 dialcohol
Benzaldehyde
Tetraphenylphosphonium

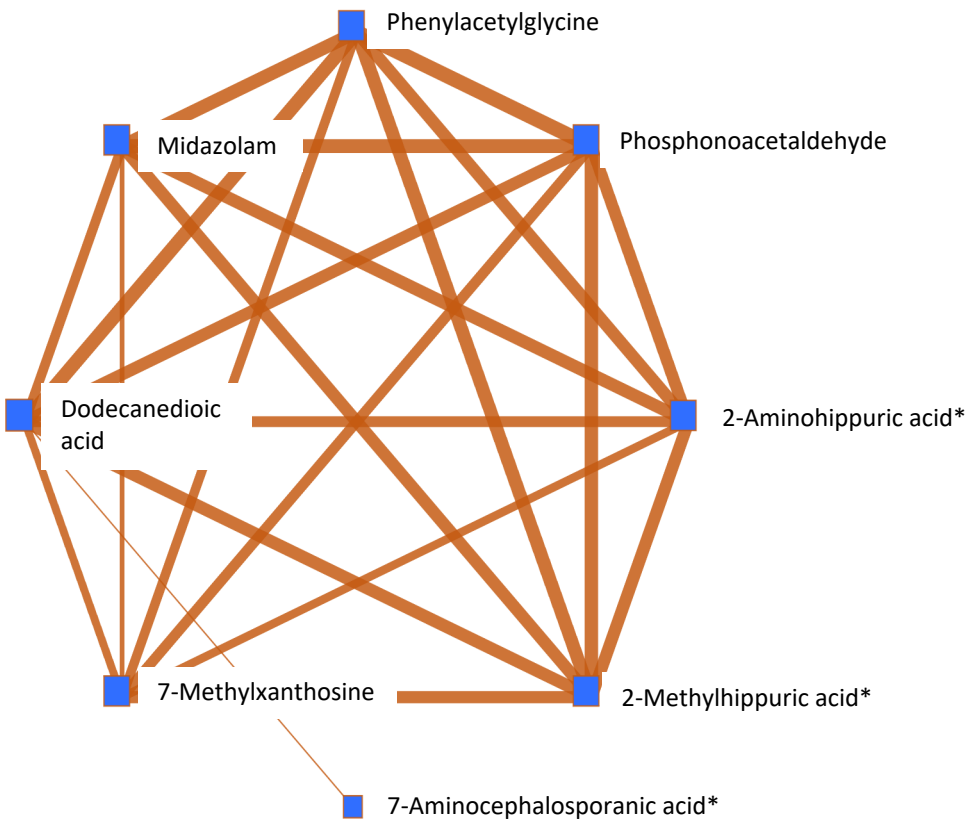
Phenylacetylglycine
Midazolam
Phosphonoacetaldehyde
Dodecanedioic acid
2-Aminohippuric acid*
7-Methylxanthosine
2-Methylhippuric acid*
7-Aminocephalosporanic acid*

a.

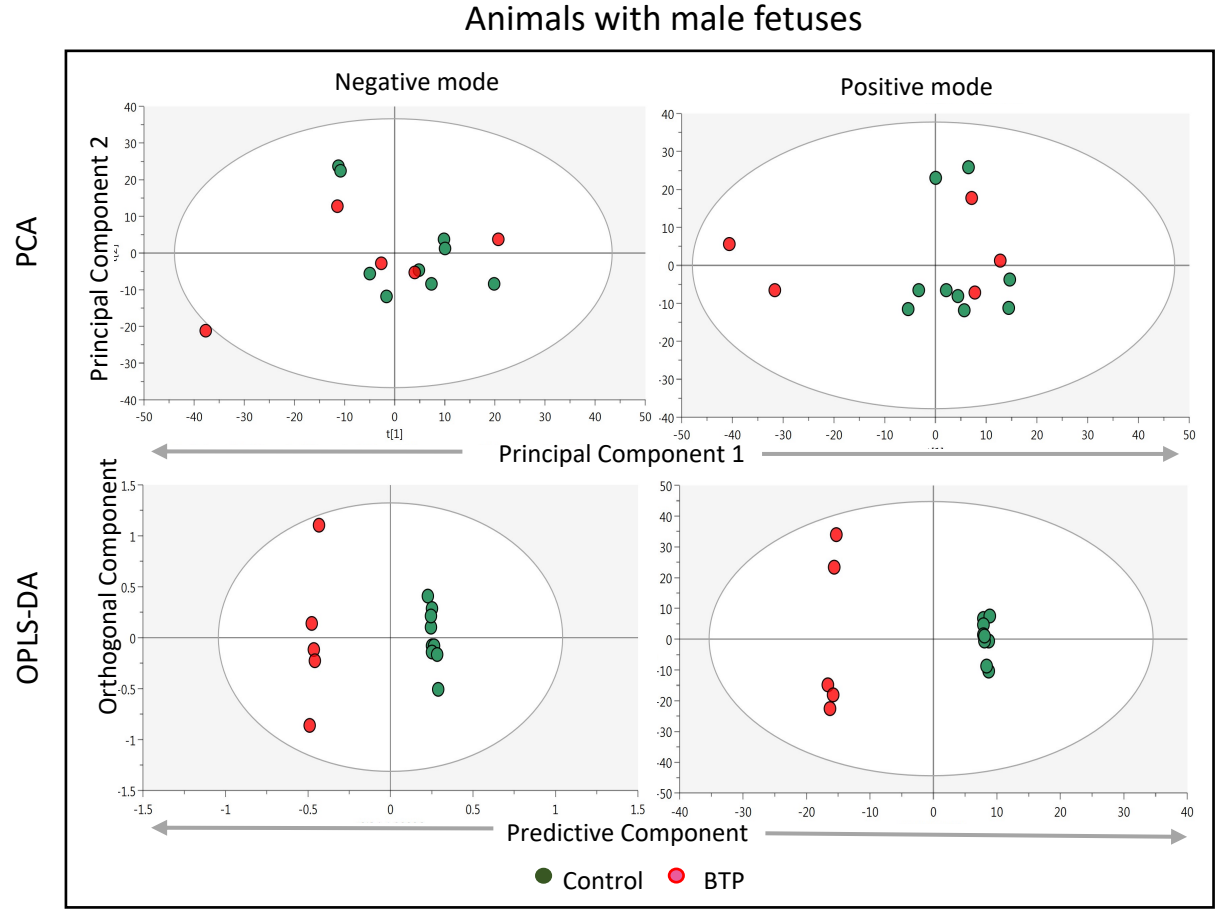
Animals with male fetuses
Negative mode
Positive mode
PCA
OPLS-DA
Principal Component 2
Principal Component 1
Orthogonal Component
Predictive Component
Control
BTP

b.

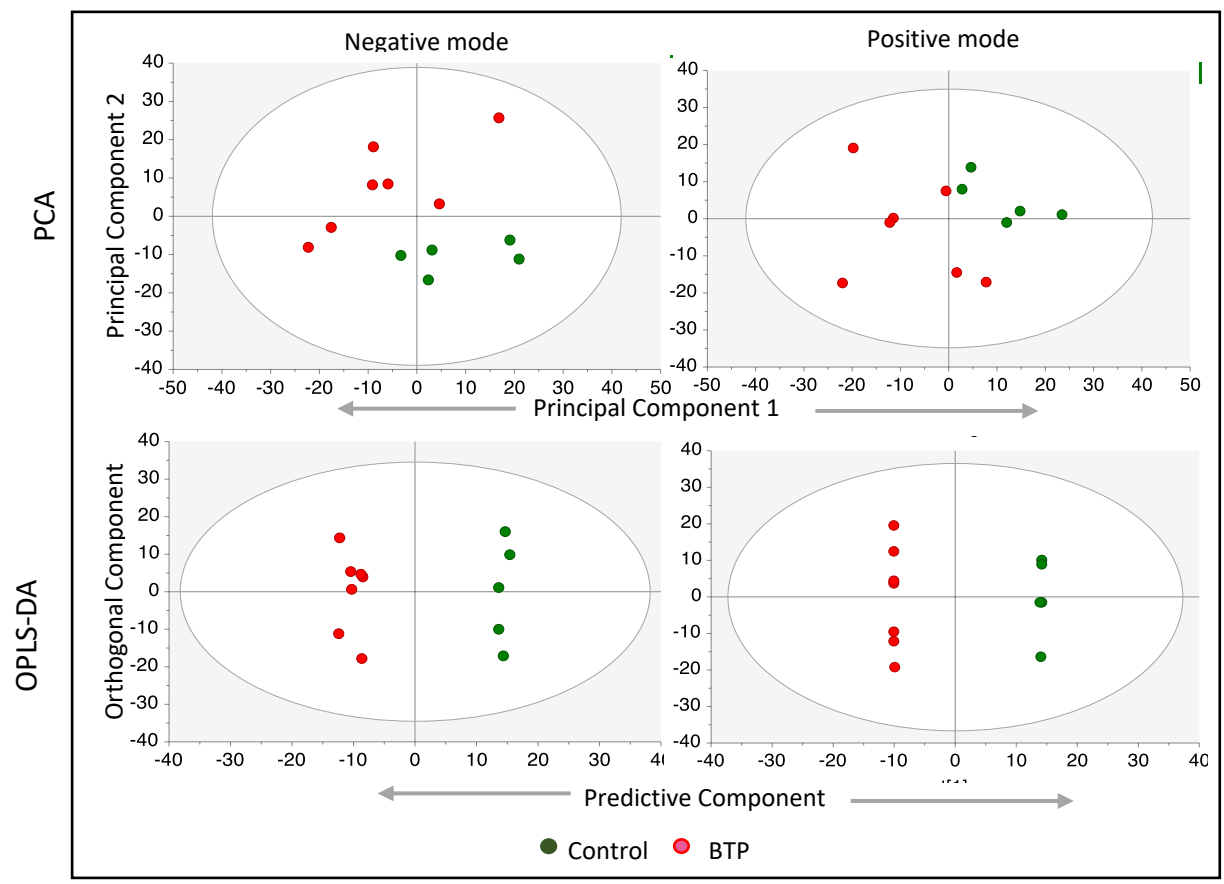
Animals with female fetuses
Negative mode
Positive mode
PCA
OPLS-DA
Principal Component 2
Principal Component 1
Orthogonal Component
Predictive Component
Control
BTP

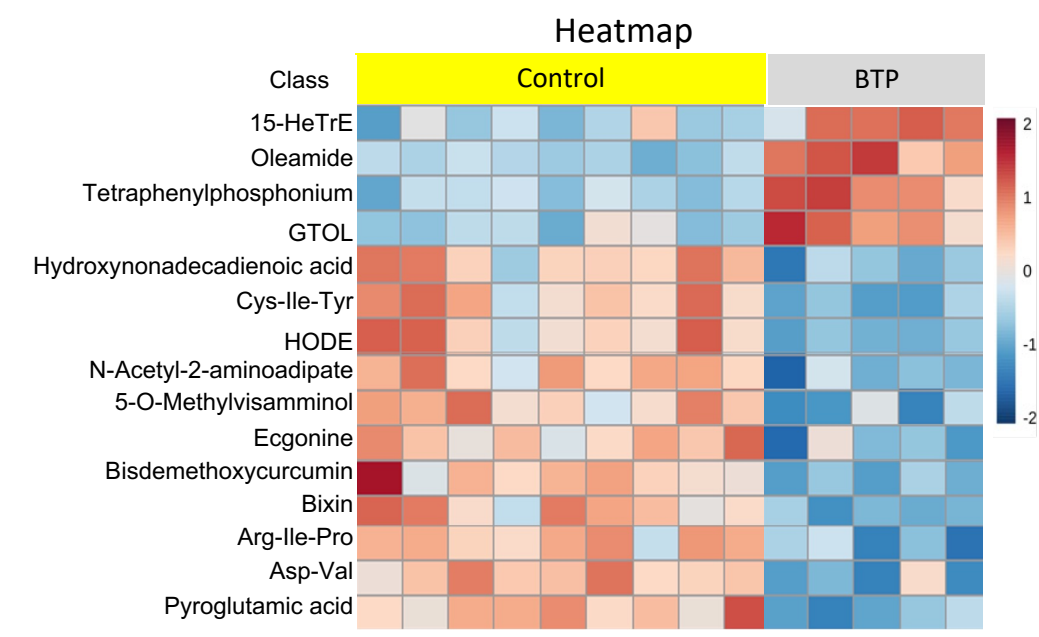
Heatmap
Class
Control
BTP
15-HeTrE
Oleamide
Tetraphenylphosphonium
GTOL
Hydroxynonadecadienoic acid
Cys-Ile-Tyr
HODE
N-Acetyl-2-aminoadipate
5-O-Methylvisamminol
Ecgonine
Bisdemethoxycurcumin
Bixin
Arg-Ile-Pro
Asp-Val
Pyroglutamic acid
2
1
0
-1
-2

Figure S9

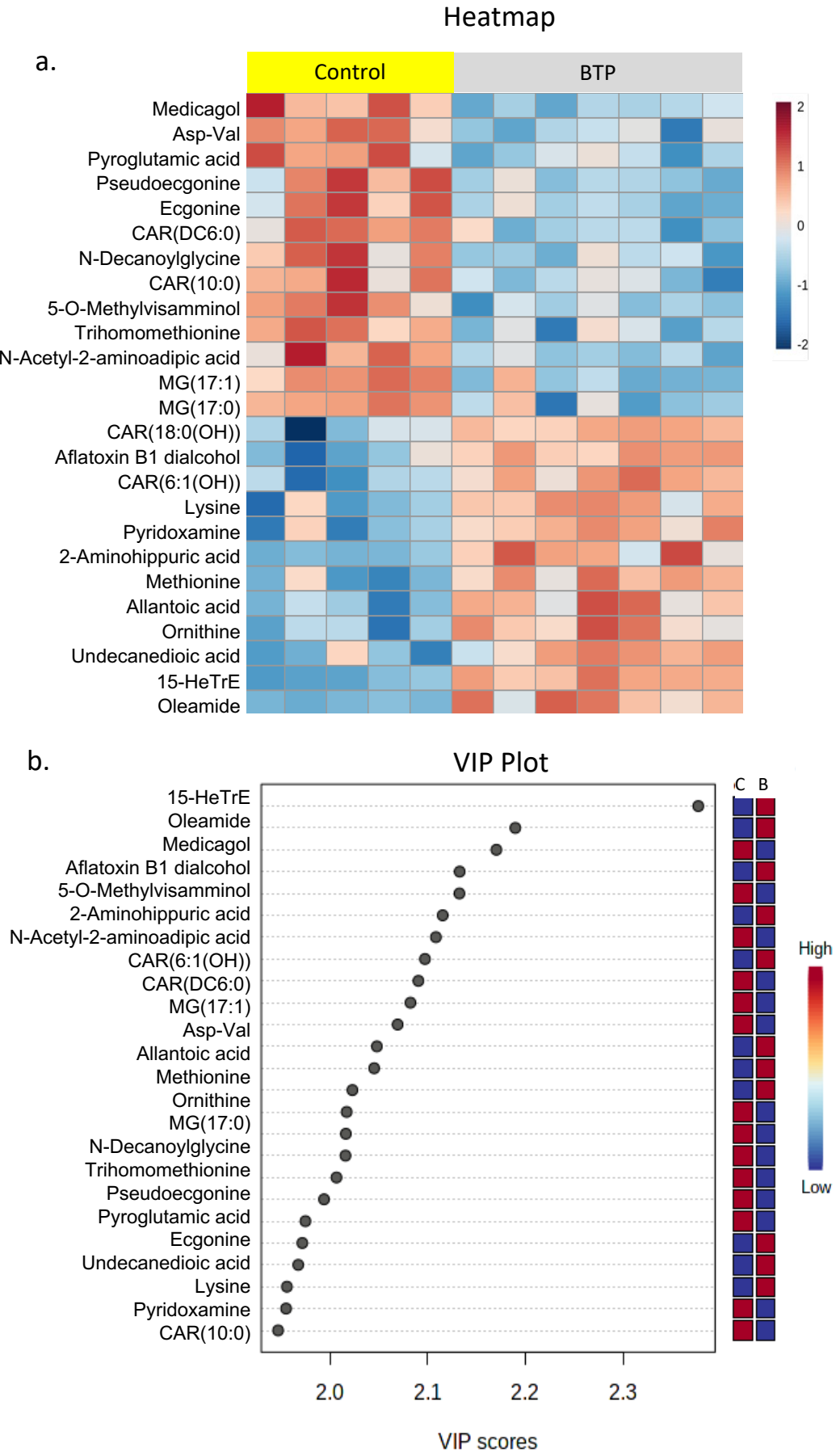
Heatmap
a.
Control
BTP
Medicagol
Asp-Val
Pyroglutamic acid
Pseudoecgonine
Ecgonine
CAR(DC6:0)
N-Decanoylglycine
CAR(10:0)
5-O-Methylvisamminol
Trihomomethionine
N-Acetyl-2-aminoadipic acid
MG(17:1)
MG(17:0)
CAR(18:0(OH))
Aflatoxin B1 dialcohol
CAR(6:1(OH))
Lysine
Pyridoxamine
2-Aminohippuric acid
Methionine
Allantoic acid
Ornithine
Undecanedioic acid
15-HeTrE
Oleamide
2
1
0
-1
-2
b.
VIP Plot
15-HeTrE
Oleamide
Medicagol
Aflatoxin B1 dialcohol
5-O-Methylvisamminol
2-Aminohippuric acid
N-Acetyl-2-aminoadipic acid
CAR(6:1(OH))
CAR(DC6:0)
MG(17:1)
Asp-Val
Allantoic acid
Methionine
Ornithine
MG(17:0)
N-Decanoylglycine
Trihomomethionine
Pseudoecgonine
Pyroglutamic acid
Ecgonine
Undecanedioic acid
Lysine
Pyridoxamine
CAR(10:0)
C
B
High
Low
2.0
2.1
2.2
2.3
VIP scores

Table 1

	Differential metabolites from Negative ion mode			Differential metabolites from Negative ion mode		
S No.	**Metabolite name**	**VIP Score**	**Adj P value**	**Metabolite name**	**VIP Score**	**Adj P value**
1	15-HeTrE	2.7	1.59E-09	Oleamide	2.6	1.28E-07
2	Methionine	2.3	1.28E-03	5-Hydroxytryptophol glucuronide	2.4	2.20E-05
3	Arg-Ile-Pro	2.3	1.13E-04	Pyroglutamic acid	2.4	3.38E-05
4	Pyroglutamic acid	2.3	1.77E-04	Asp-Val	2.2	2.10E-04
5	N-Decanoylglycine	2.3	4.73E-04	CAR(3:0(OH))	2.3	2.10E-04
6	N2-Acetyl-L-Aminoadipate	2.2	2.75E-04	Tetraphenylphosphonium	2.2	2.10E-04
7	5-Aminopentanoic acid	2.2	2.03E-03	Ecgonine	2.3	2.10E-04
8	Pseudoecgonine	2.2	5.22E-04	Ornithine	2.3	3.10E-04
9	2-Butenyl-4-methylthreonine	2.2	4.73E-04	CAR(DC6:0)	2.3	3.61E-04
10	Viridiflorine beta-lactone	2.2	1.33E-03	Lysine	2.2	3.61E-04